



## Research article

# Sulfated polysaccharides from *Caulerpa lentillifera*: Optimizing the process of extraction, structural characteristics, antioxidant capabilities, and anti-glycation properties

Suphaporn Tesvichian<sup>a</sup>, Papassara Sangtanoo<sup>b,c</sup>, Piroonporn Srimongkol<sup>b,c</sup>, Tanatorn Saisavoeay<sup>b,c</sup>, Anumart Buakeaw<sup>b,c</sup>, Songchan Puthong<sup>b,c</sup>, Sitanan Thitiprasert<sup>b,c</sup>, Wanwimon Mekboonsonglarp<sup>d</sup>, Jatupol Liangsakul<sup>d</sup>, Anek Sopon<sup>e</sup>, Mongkhon Prawatborisut<sup>f</sup>, Onrapak Reamtong<sup>g</sup>, Aphichart Karnchanatat<sup>b,c,\*</sup>

<sup>a</sup> Program in Biotechnology, Chulalongkorn University, 254 Phayathai Road, Wangmai, Pathumwan, Bangkok, 10330, Thailand

<sup>b</sup> Institute of Biotechnology and Genetic Engineering, Chulalongkorn University, 254 Phayathai Road, Wangmai, Pathumwan, Bangkok, 10330, Thailand

<sup>c</sup> Center of Excellence in Bioconversion and Bioseparation for Platform Chemical Production, Institute of Biotechnology and Genetic Engineering, Chulalongkorn University, 254 Phayathai Road, Wangmai, Pathumwan, Bangkok, 10330, Thailand

<sup>d</sup> Scientific and Technological Research Equipment Centre, 254 Phayathai Road, Wangmai, Pathumwan, Bangkok, 10330, Thailand

<sup>e</sup> Aquatic Resources Research Institute, 254 Phayathai Road, Wangmai, Pathumwan, Bangkok, 10330, Thailand

<sup>f</sup> Bruker Switzerland AG, 175, South Sathorn Road, 10th Floor, Sathorn City Tower, Thungmahamek, Sathorn, Bangkok, 10120, Thailand

<sup>g</sup> Department of Molecular Tropical Medicine and Genetics, Mahidol University, 420/6 Ratchawithi Road, Ratchathewi, Bangkok, 10400, Thailand

## ARTICLE INFO

## Keywords:

*Caulerpa lentillifera*  
Sulfated polysaccharide  
Antioxidant  
Anti-Glycation

## ABSTRACT

The polysaccharides found in *Caulerpa lentillifera* (sea grape algae) are potentially an important bioactive resource. This study makes use of RSM (response surface methodology) to determine the optimal conditions for the extraction of valuable SGP (sea grape polysaccharides). The findings indicated that a water/raw material ratio of 10:1 mL/g, temperature of 90 °C, and extraction time of 45 min would maximize the yield, with experimentation achieving a yield of 21.576 %. After undergoing purification through DEAE-52 cellulose and Sephadex S-100 column chromatography, three distinct fractions were obtained, namely SGP<sub>11</sub>, SGP<sub>21</sub>, and SGP<sub>31</sub>, each possessing average molecular weights of 38.24 kDa, 30.13 kDa, and 30.65 kDa, respectively. Following characterization, the fractions were shown to comprise glucose, galacturonic acid, xylose, and mannose, while the sulfate content was in the range of 12.2–21.8 %. Using Fourier transform infrared spectroscopy (FT-IR) it was possible to confirm with absolute certainty the sulfate polysaccharide attributes of SGP<sub>11</sub>, SGP<sub>21</sub>, and SGP<sub>31</sub>. NMR (nuclear magnetic resonance) findings made it clear that SGP<sub>11</sub> exhibited α-glycosidic configurations, while the configurations of SGP<sub>21</sub> and SGP<sub>31</sub> were instead β-glycosidic. The *in vitro* antioxidant assays which were conducted revealed that each of the fractions was able to demonstrate detectable scavenging activity against 1,1-diphenyl-2-picrylhydrazyl (DPPH) radicals and 2,2'-azino-bis (3-ethylbenzothiazoline-6-sulfonic acid) (ABTS) radical cations. All fractions were also found to exhibit the capacity to

\* Corresponding author. Center of Excellence in Bioconversion and Bioseparation for Platform Chemical Production, Institute of Biotechnology and Genetic Engineering, Chulalongkorn University, 254 Phayathai Road, Wangmai, Pathumwan, Bangkok, 10330, Thailand.

E-mail address: [Aphichart.K@chula.ac.th](mailto:Aphichart.K@chula.ac.th) (A. Karnchanatat).

scavenge NO radicals in a dose-dependent manner. SGP<sub>11</sub>, SGP<sub>21</sub>, and SGP<sub>31</sub> were also able to display cellular antioxidant activity (CAA) against the human adenocarcinoma colon (Caco-2) cell line when oxidative damage was induced. The concentration levels were found to govern the extent of such activity. Moreover, purified SGP were found to exert strong inhibitory effects upon glycation, with the responses dependent upon dosage, thus confirming the potential for SGP to find a role as a natural resource for the production of polysaccharide-based antioxidant drugs, or products to promote improved health.

## 1. Introduction

Polysaccharides are pivotal natural macromolecules within the body, renowned for their distinctive physical and chemical attributes, as well as their diverse range of biological activities. These activities encompass immunomodulation, antitumor effects, anti-oxidative properties, antihyperglycemic benefits, antiglycation capabilities, and antifatigue functions [1,2]. In recent years, marine macroalgae have emerged as a fascinating source of functional foods, primarily due to their rich mineral content, essential amino acids, and dietary fibers. Moreover, these algae harbor an array of bioactive compounds, including polysaccharides, proteins, and lipids, albeit with varying content levels (ranging from 4 % to 76 % of the dry weight for polysaccharides and 5 %–47 % of the dry weight for proteins) [3]. Furthermore, variations in monosaccharide composition, molecular chain length and orientation, branching, and connections with functional groups may complicate the structures of polysaccharides and their potential bioactivities [4]. Therefore, the complex nature of marine algal polysaccharides keeps attracting researchers' interest and open up new avenues for the development of novel functional foods and medicinal applications.

*Caulerpa lentillifera*, an edible marine macroalgae, is also known as sea grapes or green caviar and belongs to the Caulerpa genus. It thrives in tropical and subtropical coastal regions worldwide, with particular abundance in Southeast Asia and the broader Indo-Pacific area [5,6]. Edible algae possess a unique composition, offering a multitude of beneficial properties, which account for their popularity in Southeast Asian cuisine. Sea grape algae boasts high nutritional value due to its rich protein content, essential amino acids, soluble carbohydrates, polyunsaturated fatty acids (PUFA), minerals, ash, vitamins, and pigments. Additionally, it exhibits antioxidant capabilities attributed to its polyphenol content [7]. The utilization of algae often revolves around their functional components, used in the production of "healthy" foods with potential positive effects on specific medical conditions [8,9].

Sea grape algae polysaccharides (SGP) are considered especially important because of the structural features and the resulting functional properties. The composition involves a linked structure of repeating sugar units. These complex carbohydrates contain unique monosaccharide arrangements, based on mannose (Man), glucose (Glu), galactose (Gal), xylose (Xyl), and rhamnose (Rha). The biological and physicochemical properties of SGP are dependent upon the precise way these monosaccharides are arranged in the polysaccharide chain [10]. Studies have demonstrated that SGP offer various bioactivities, including anticancer [11,12], antioxidant [13,14], anticoagulant [15,16], immune-stimulatory [17,18], anti-tumor [19], anti-virus [20], and anti-inflammatory properties [21, 22]. The literature explains that these qualities were identified in studies which made use of water or ethanol sea grape algae extracts, and these mixtures are rather complex and typically contain a wide range of active components. Notably, sulfated polysaccharides isolated from *C. lentillifera* have been reported to possess antioxidant properties [13], demonstrate anti-diabetic effects [23], exhibit anticancer activities [24], and even show anti-SARS-CoV-2 activity [20].

A number of researchers have examined the structural attributes and biological activities of purified polysaccharides obtained from sea grape algae, but there has been little research into the optimal extraction conditions. This research applies response surface methodology (RSM) to examine the aforementioned process in order to gain a more comprehensive understanding of how the extraction rate of the polysaccharides is influenced by variables such as extraction temperature, time, and the water-to-raw material ratio. Column chromatography was used for the initial purification of the polysaccharide extract, while determination of the structure was achieved through spectroscopic and chemical techniques. The influence of SGP upon antioxidant activity was also evaluated, in this case using chemical antioxidant tests and a cellular antioxidant assay. Meanwhile, the use of a bovine serum albumin-glucose glycation system *in vitro* allowed the antiglycation effects to be estimated, ultimately bringing about a better understanding of the polysaccharides of sea grape algae, and their potential applications in the pharmaceutical or food sectors.

## 2. Materials and methods

### 2.1. Biological materials

Sea grape algae were cultivated under controlled conditions at Family Farm, Ban Laem District, Phetchaburi, Thailand (N 13° 01' 37.2"; E 100° 04' 42.8"), and harvested in August 2019. After collection, the algae underwent rinsing in seawater and brushing to eliminate macroscopic epiphytes and sand particles. Further cleansing with tap water removed residual salt, followed by air drying for 4 days at 25 °C and thermostat drying for 12 h at 60 °C. The dried algae were manually crushed, powdered using a grinder, and the powder's moisture content determined to be 12–15 % by dry weight. The powder was stored in dark bags to avoid light and moisture. The human intestinal epithelial cell line, Caco-2 cells (ATCC® HTB-37™), provided by the American Type Culture Collection (ATCC, Manassas, VA, USA), was cultured in Eagle's Minimum Essential Medium (EMEM) supplemented with L-glutamine and 10 % FBS (fetal bovine serum) from Gibco (Rockville, MD, USA). These cells were incubated under 5 % carbon dioxide at 37 °C in a humidified

chamber.

## 2.2. Chemical materials

2, 2'-azino-bis(3-ethylbenzothiazoline-6-sulfonic acid) (ABTS), aminoguanidine (AG), bovine serum albumin (BSA), Barium chloride ( $\text{BaCl}_2$ ), 2,2-diphenyl-1-picrylhydrazl (DPPH), 2',7'-Dichlorodihydrofluorescein diacetate (DCFH-DA), 3-(4,5-dimethyl-2-thiazolyl)-2,5-diphenyl-2H-tetrazolium bromide (MTT), Dimethyl sulfoxide, (DMSO), monosaccharides standards including: Arabinoose (Ara), Fructose (Fru), Galactose (Gal), Glucose (Glc), Galacturonic acid (GalA), Ribose (Rib), Mannose (Man), and Xylose (Xyl), N, N'-methylenebis (acrylamide), naphthylethylenediamine dichloride (NED;  $\text{C}_{12}\text{H}_{16}\text{Cl}_2\text{N}_2$ ), nitrotetrazolium blue chloride (NBT), sodium nitroprusside (SNP;  $\text{C}_5\text{FeN}_6\text{Na}_2\text{O}$ ), and all other reagents and chemicals were of analytical grade obtained from Sigma-Aldrich, Merck (St. Louis, MO, USA). Thermo Fisher Scientific (San Jose, CA, USA) provided ethanol, acetonitrile (ACN), N,N,N',N'-Tetramethyl ethylenediamine (TEMED), formic acid, and trifluoroacetic acid (TFA), which were of chromatographic grade. Cleaver Scientific (Rugby, UK) provided Blue ultra pre-stained protein ladder (6.5–270 kDa).

## 2.3. Single factor testing

Testing was carried out to determine the influence of the water-to-raw material ratio, extractions time, and extraction temperature upon the crude polysaccharide yield. Dry sea grape algae were extracted via the process of double-distilled water (dd $\text{H}_2\text{O}$ ) autoclave extraction. A variety of solutions and materials were used in differing ratios (5:1, 10:1, 15:1, 25:1, and 45:1), and for differing extraction times (15 min, 45 min, 60 min, and 90 min), and differing extraction temperatures (60 °C, 70 °C, 80 °C, and 90 °C) at 1.5 lbs with autoclave (HVA-110; Hirayama Manufacturing Co., Ltd., Tokyo, Japan). The Sevag reagent method was employed for the de-proteinization of the supernatant [25], and the liquid obtained underwent overnight dialysis against dd $\text{H}_2\text{O}$  in a dialysis bag whereby the cut-off was set to 3500 Da. Freeze drying was carried out to allow the crude polysaccharide to be obtained. The crude polysaccharide yield was determined from Equation (1) as shown below:

$$\text{Yield (\%, w / w)} = \frac{\text{Weight of crude polysaccharide (g)}}{\text{Weight of algal powder (g)}} \times 100 \quad (1)$$

## 2.4. Experimental design and statistical analysis

In order to determine the ideal polysaccharide extraction conditions, RSM and CCD (central composite design) were utilized. Autoclave extraction was carried out while the variables under investigation were adjusted: temperature ranged from 60 °C to 100 °C, extraction time from 35 to 55 min, and the volume ratio of dd $\text{H}_2\text{O}$  to raw material ranged from 5 mL to 15 mL. Early outcomes set the initial factor range. The extraction process covers five levels which are represented by the designated values of -2, -1, 0, 1, 2 which respectively indicate very low, low, medium, high, and very high levels. This can be seen in Table 1. The mean polysaccharide percentage for the extraction levels from three trials serves as the response variable given as Y. In total, 17 trials were performed, encompassing 3 center points, 6 axial points, and 8 factorial points, as can be observed in Table 2. The resulting response variables were then used in the general equation as a second-order polynomial which is shown below as Equation (2):

$$Y = \beta_0 + \sum_{i=1}^k \beta_i X_i + \sum_{i=1}^{k-1} \sum_{j=i+1}^k \beta_{ij} X_i X_j + \sum_{i=1}^k \beta_{ii} X_i^2 + \epsilon \quad (2)$$

where  $X_i$  and  $X_j$  serve as input variables ( $i \neq j$ ) affecting the response denoted as Y, and  $\beta_0$  represents the offset term. The regression coefficients ( $\beta_i$ ), ( $\beta_{ij}$ ), and ( $\beta_{ii}$ ) indicate the linear, interaction, and quadratic terms, while k and  $\epsilon$  respectively serve as the number of variables and number of residuals in each trial. The design and analysis of RSM required the use of Design-Expert v11.0.5 software, while the correlation coefficient ( $R^2$ ), adjusted determination coefficient (Adj- $R^2$ ), and adequate precision were employed as a means of assessing the overall suitability of the model. For the consideration of accuracy, a p-value <0.05, lack of fit p-value >0.05,  $R^2 > 0.9$ , and adequate precision >4 were deemed necessary. A test was carried out to determine the significance of the differences between means by using analysis of variance (ANOVA), while the optimal conditions were selected on the basis of the experiments achieving the greatest SGP yield. For the remainder of this study, all SGP were produced by applying these optimal conditions in order to achieve maximum yields while minimizing the time and cost.

**Table 1**

Independent variables and polysaccharide coded levels on the basis of CCD.

Independent variables	Coded levels				
	-2	-1	0	+1	+2
A: temperature (°C)	60	70	80	90	100
B: time (min)	35	40	45	50	55
C: water volume (mL)	5	7.5	10	12.5	15

**Table 2**

CCD findings for the response variable values, encompassing both actual and predicted yields of polysaccharides under different reaction conditions for the three independent variables (A, B, C).

Run	Space Type	Coded independent variable levels			Yield of SGP (g/100 g)	
		A	B	C	Actual Value	Predicted Value
1	Factorial	+1	-1	-1	1.292	1.2900
2	Factorial	-1	+1	-1	0.730	0.7794
3	Axial	-2	0	0	0.480	0.4343
4	Axial	0	+2	0	0.950	0.8996
5	Axial	0	0	-2	0.774	0.7653
6	Factorial	+1	-1	+1	1.087	1.0800
7	Axial	0	0	+2	0.440	0.4048
5	Factorial	-1	-1	+1	0.600	0.6342
9	Factorial	+1	+1	+1	1.221	1.2600
10	Center	0	0	0	1.571	1.5600
11	Center	0	0	0	1.593	1.5600
12	Factorial	-1	+1	+1	0.580	0.6267
13	Center	0	0	0	1.564	1.5600
14	Axial	+2	0	0	1.420	1.4200
15	Factorial	+1	+1	-1	1.310	1.3200
16	Factorial	-1	-1	-1	0.930	0.9349
17	Axial	0	-2	0	0.870	0.8766

## 2.5. SGP purification

Crude SGP (~250 mg) was dissolved in 5 mL of distilled water (ddH<sub>2</sub>O). A DEAE-cellulose fast flow column (1.6 × 20 cm, HiMedia, USA) was employed for elution with ddH<sub>2</sub>O and varying NaCl concentrations (0.3, 0.6, 0.9, 0.4, and 1.2 M). A vacuum pump adjusted the column flow rate (2 mL/min) when necessary. The phenol-sulfuric acid assay measured all fractions, with 10 mL fractions assayed for sugars. Sugar-containing fractions underwent additional purification by pooling and lyophilization. Subsequently, a 50 mg SGP sample was prepared, dissolved in 5 mL of ddH<sub>2</sub>O, and further purified using a Sephadex S-100 HR column (1.6 × 60 cm, GE Healthcare, Sweden). Elution occurred with ddH<sub>2</sub>O at 0.5 mL/min, collecting 5 mL fractions, and assaying sugar content with the phenol-sulfuric acid method. Those fractions which were identified to contain sugar were pooled and allowed to condense, before dialysis for 24 h using flowing ddH<sub>2</sub>O for the purpose of salt removal. Once purified, the SGP was collected, lyophilized, and placed into storage at a temperature of 4 °C.

## 2.6. Analysis of chemical composition

### 2.6.1. Carbohydrate content

The phenol-sulfuric acid method allowed the determination of the carbohydrate content with glucose serving as the standard [26]. Initially, a mixture is created using 0.2 mL of polysaccharide solution and 0.8 mL of phenol solution (5 % w/v) combined with 2.5 mL of concentrated sulfuric acid. The resulting mixture is then incubated at room temperature in darkness for 30 min, before absorbance measurement is taken at 490 nm by microplate reader (Thermo Multiskan FC, Thermo Fisher Scientific Inc., USA). A standard curve can then be created using a series of glucose concentrations.

### 2.6.2. Monosaccharide content

The purified SGP fractions underwent acid hydrolysis at 80 °C for 6 h with 2 mL TFA (2 M). A rotating vacuum evaporator was then used to remove any residual TFA. The aqueous phase was then passed through a 0.22 m microporous filter prior to HPLC (high performance liquid chromatography) analysis. The monosaccharides in the various fractions were identified via the standard elution times, with contents found to include Ara, Fru, Gal, GalA, Glc, Man, Rib, and Xyl. HPLC confirmed these results via RI (refractive index) detection at 37 °C utilizing a BP-800 H column (Benson Polymeric, USA). Finally, elution using HPLC grade water was performed using the flow rate of 0.5 mL/min.

### 2.6.3. Sulfate content

The sulfate content of purified SGP fractions was assessed using the barium chloride-gelatin method [27]. Hydrolysis with 1 M hydrochloric acid, rotary evaporation, dissolution in 1 mL water, and reaction with 5 % barium chloride-gelatin and 8 % TCA followed. Absorbance at 360 nm, after 20 min of incubation at room temperature, was measured, referencing a standard curve with sodium sulfate solution.

## 2.7. MW analysis

The MW of SGP was assessed through a modified approach based on the work of Srimongkol et al. [28], using GPC (gel-permeation chromatography) (Waters, USA) with a 2414 RI detector and four PWXL columns of TSK-gel (TOSOH, Japan) connected in series. The

purified SGP (2 mg/mL) was initially filtered *via* 0.2 µm nylon filter, whereupon the sample solutions (20 µL) and standards were independently injected prior to elution using HPLC grade water at a flow rate of 1 mL/min at a steady 40 °C. Various MW pullulans ranging from 6 kDa to 805 kDa acted as the standard, with 12 kDa Dextan obtained from Sigma (St. Louis, Missouri, USA) enabling the system accuracy to be verified on a daily basis.

## 2.8. FT-IR (fourier transform infrared) spectrometry

Semi-solid purified SGP (4 mg/mL) was tested by recording the Fourier transform infrared spectroscopy (FT-IR) spectra, using a pressure arm to ensure sufficient quality of the spectra by maintaining adequate contact between the diamond/ZnSe crystal and the sample. This approach allows identification of the organic functional groups of the polysaccharides when examining the spectrophotometer range of 4000 to 515 cm<sup>-1</sup> using an FT-IR infrared spectrometer (PerkinElmer, Spectrum GX 2000 (Boston, USA) and Nicolet 400D, (California, USA Instruments).

## 2.9. NMR (nuclear magnetic resonance) spectrometry

NMR spectrometry was performed by initially placing ~60 mg of polysaccharide inside the NMR tube, dissolved in 0.5 mL of D<sub>2</sub>O. The NMR spectra can then be recorded using a Bruker Avance Ascend (600.15 MHz for <sup>1</sup>H and 150.91 MHz for <sup>13</sup>C) spectrometer (Bruker, Germany) at 60 °C, producing one-dimensional (1D <sup>1</sup>H NMR and <sup>13</sup>C NMR) and two-dimensional (2D H–H COSY, HSQC, and HMBC) results. For <sup>1</sup>H NMR experiments the parameters were: a spectral width of 11.9 kHz, a 30° pulse angle, an acquisition time of 2.8 s, a relaxation delay of 1.5 s, for 512 scans. For 150 MHz proton decoupled <sup>13</sup>C NMR experiments the parameters were: a spectral width of 35.7 kHz, a 30° pulse angle, an acquisition time of 0.92 s, a relaxation delay of 2.0 s, for 25,600 scans. MestReNova-11.0.2 software was employed to process the data findings. For terminology, HMBC = heteronuclear multiple-bond correlation; H–H COSY = hydrogen-hydrogen correlation spectroscopy, and HSQC = heteronuclear single quantum coherence.

## 2.10. Antioxidant activity

### 2.10.1. ABTS and DPPH radical scavenging activities assay

Free radical scavenging activity was assessed through ABTS and DPPH assays following Saisavoye et al. [29]. For the DPPH assay, samples were mixed with 100 µM DPPH solution (1:4, v/v) and incubated in darkness for 15 min at room temperature. Absorbance at 517 nm was measured using a microplate reader. In the ABTS assay, a solution was prepared by mixing 2.45 mM potassium persulphate with 7 mM ABTS (1:1, v/v) and incubating for 12 h. After dilution, the absorbance at 734 nm was adjusted to 0.7 ± 0.02. Mixing the sample with activated ABTS solution (1:30, v/v) and incubating for 10 min at room temperature preceded absorbance measurement at 734 nm. Ascorbic acid (100 µg/mL) served as the positive control.

### 2.10.2. Nitric oxide (NO) radical scavenging activity assay

The nitric oxide (NO) radical scavenging activity was assessed using a technique proposed by Suttisawan et al. [30]. Nitric oxide radicals were generated by converting nitrite ions from an SNP solution, and the Griess reaction was employed for assessment. Sample dilutions (50 µL) were mixed with 10 mM SNP in pH 7.2 phosphate buffer, incubated for 2.5 h at room temperature in light conditions. Subsequently, 200 µL of 0.33 % (w/v) sulphanilamide (in 5 % (v/v) phosphoric acid) and 200 µL of 0.1 % (w/v) NED were added, followed by 30 min of incubation at room temperature. Absorbance was measured at 540 nm, with ascorbic acid (100 µg/mL) as the positive control.

### 2.10.3. Calculations of percentage inhibition

The radical scavenging percentage can be calculated by the application of Equation

$$\left[ \frac{(\text{Abs}_{\text{control}} - \text{Abs}_{\text{blank}}) - (\text{Abs}_{\text{sample}} - \text{Abs}_{\text{background}})}{(\text{Abs}_{\text{control}} - \text{Abs}_{\text{blank}})} \right] \times 100 \quad (3)$$

where  $\text{Abs}_{\text{control}}$  showed the control absorbance (no sample),  $\text{Abs}_{\text{sample}}$  represented the polysaccharide samples absorbance,  $\text{Abs}_{\text{blank}}$  represented the deionized water absorbance, and  $\text{Abs}_{\text{background}}$  represented the color absorbance of the samples. The IC<sub>50</sub> value, indicating the polysaccharide concentration required to achieve the 50 % inhibition of antioxidant activity, was established with GraphPad Prism v. 6.01 software for Windows (GraphPad Software Inc., San Diego, CA, USA).

## 2.11. CAA (cellular antioxidant activity) assay

### 2.11.1. Cytotoxicity activity of the purified SGP

After establishing the free radical scavenging abilities of the SGPs, their potential cytotoxic effects on the Caco-2 (human adenocarcinoma colon) cell line were assessed *in vitro*. Cell suspensions in complete medium (EMEM with 10 % v/v FBS) were diluted and plated ( $5 \times 10^3$  cells/well) in 96-well plates (200 µL/well, absorbance at 540 nm = 1.0). Incubation occurred at 37 °C for 72 h under 5 % carbon dioxide. Fresh CM with various SGP concentrations replaced the cell culture medium for another 72-h incubation. Subsequently, 10 µL of 5 mg/mL MTT in normal saline was added to each well, and the mixture incubated for 4 h. Media removal,

addition of 150 µL DMSO per well to dissolve the resulting formazan crystals, and measurement of absorbance at 540 nm using a microplate reader followed. The absorbance value at 540 nm was considered proportional to viable cells, allowing the calculation of relative percentage cell viability using Equation (4).

$$\text{Cell survival (\%)} = \text{Abs}_{\text{sample}} / \text{Abs}_{\text{control}} \times 100 \quad (4)$$

in which the control, containing no sample was predetermined to represent cell survival of 100 %. The data were then employed to determine the IC<sub>50</sub> value from GraphPad Prism version 6.01. The assays were all carried out in triplicate.

### 2.11.2. CAA

The technique proposed by Wolfe and Liu [31] was employed to test the purified SGP fractions to determine the *in vitro* CAA in Caco-2 cells. Initially, the Caco-2 cells were seeded in a 96-well plate at a density of  $6 \times 10^4$  cells per well in culture medium before incubation for 24 h to achieve 90–100 % confluence, verified by microscope. To ensure that the plate location did not influence the results, the outer wells were not used. Upon reaching confluence, the growth medium was removed, before rinsing the cells in sterile 20 mM phosphate buffer saline (PBS; pH 7.4) in order to eliminate dead or non-adherent cells. Various concentrations of purified SGP fractions were then prepared, and 100 µL was placed in each well, whereupon 50 µL of 50 µM DCFH-DA probe solution was added. The cells then underwent incubation at 37 °C for 1 h, before removing the treatment solutions and thrice washing the cells in 100 µL of PBS. The final step involved the addition of 100 µL of 500 µM ABAP solution to each well, with the exception of the negative control and blank wells. Measurements of the fluorescence emitted at 528 nm following excitation at 485 nm were taken using a microplate reader at 5-min intervals for a period of 90 min while the temperature was maintained at 37 °C. Equation (5) below shows the calculation of the percentage reduction, or CAA unit:

$$\text{CAA Unit} = \% \text{reduction} = (1 - \text{AUC}_{\text{sample}} / \text{AUC}_{\text{control}}) \times 100 \quad (5)$$

in which AUC<sub>sample</sub> represents the integrated area below the curve indicating sample fluorescence vs. time, and AUC<sub>control</sub> represents the integrated area below the control curve for quercetin obtained from the triplicate findings of four independent trials in the form of mean ± standard error.

## 2.12. Antiglycation activity assay

### 2.12.1. Non-enzymatic protein glycation

Protein glycation was carried out *in vitro* in line with the approach of Wang et al. [32], by first of all preparing a mixture of BSA (20 mg/mL, 10 mL), glucose (500 mM, 5 mL), 0.02 % sodium azide, and phosphate buffer (200 mM, pH 7.4). To determine the anti-glycation properties, BSA was incubated with Glu while the purified SGP fractions (0.5 mg/mL) were present. Incubation followed for 28 days at 37 °C in an incubator shaker. On the 7th, 14th, 21st, and 28th days of incubation, the anti-advanced glycation end products (aAGE) were removed. Testing of the AGEs followed the procedures set out in the sections which follow, while for a control, BSA solution was prepared in the absence of Glu but incubated under the same protocol. The positive control was 0.5 mg/mL of AG, since it is well-known to be an anti-glycation agent. Finally, SDS-polyacrylamide gel electrophoresis (SDS-PAGE) was used to detect the glycated material (5 µL; 28th day).

### 2.12.2. Spectrophotometric analysis of the NBT reductive assay

The NBT reductive assay was carried out in line with the method proposed by Baker [33], requiring a reaction mixture comprising 2.0 mL NBT reagent (0.3 mM) and 0.5 mL glycated material in a sodium carbonate buffer (100 mM, pH 10.35). The mixture was incubated at room temperature for 15 min, before the absorbance was measured at 530 nm. The inhibition percentage could then be calculated using Equation (3), for the initial stages of protein glycation.

### 2.12.3. Spectrophotometric analysis of the Girard-T assay

The Girard-T assay [30] allows spectrophotometric measurement of the dicarbonyl compounds to be carried out. The procedure begins with the incubation of 0.4 mL of the glycated material at room temperature for 1 h mixed with 0.2 mL Girard-T stock solution (500 mM) and 3.4 mL sodium formate (500 mM, pH 2.9). The absorbance is then measured at 294 nm using a UV-Visible (1800 PC) spectrophotometer (Shimadzu Corporation, Kyoto, Japan). The result is duly compared to a blank sample which comprises all of the reagents with the exception of the Girard-T stock solution. This allows a calibration curve to be produced which uses glyoxal as the standard. The curve then allows further calculation of the yields of the dicarbonyl compounds in the intermediate phase, while the percentage inhibition for the intermediate protein glycation phase is calculated using Equation (3).

### 2.12.4. Analysis of AGEs

The maximum wavelengths for the excitation and emission of the glycated material were evaluated by scanning using a spectrofluorophotometer, with the respective resulting values of 370 nm and 450 nm being determined. The assessment was performed by initially diluting 0.5 mL of the glycated material to 10 mL with distilled water before measuring the value for FI (fluorescent intensity). The scavenging activity was then determined as a percentage in the final protein glycation phase by applying Equation (6), as shown below:

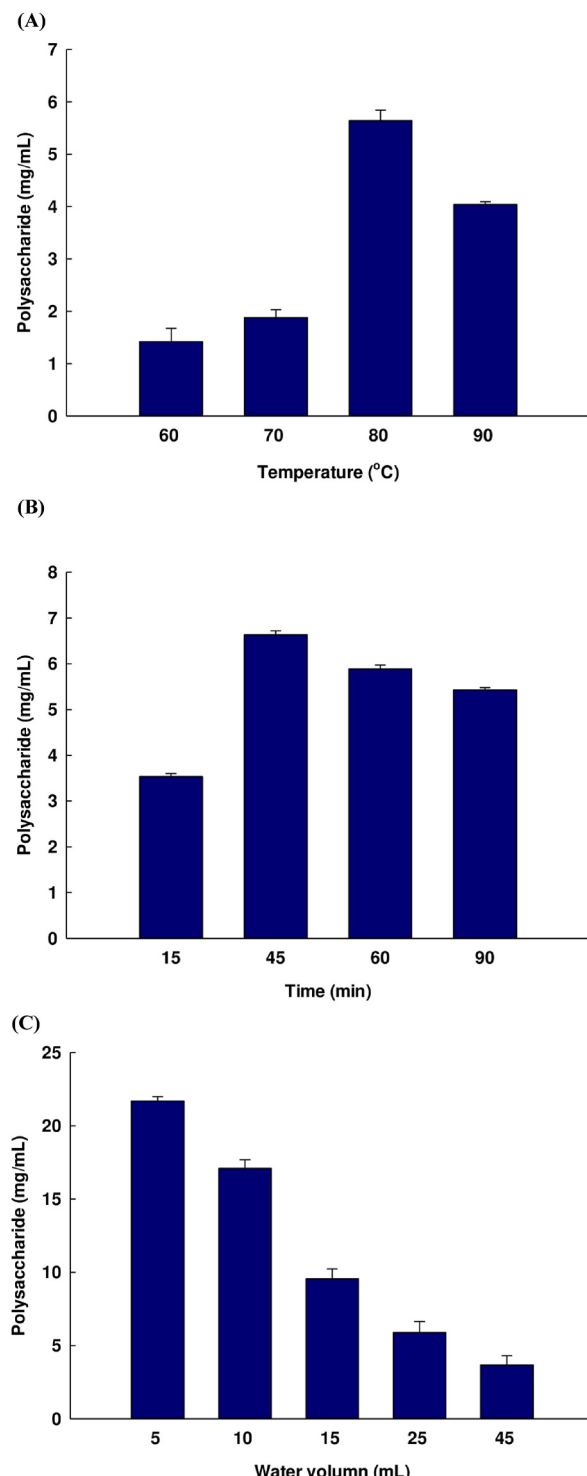


**Fig. 1.** Outcomes from single-factor experimentation upon SGP extraction yields. Single factor experiments were performed to determine the optimal extraction temperature (A), extraction time (B), and ratio of water volume to raw material (C) upon the polysaccharide yield. One factor varied while the others remained constant in each trial. Data were presented as mean  $\pm$  SD ( $n = 3$ ).

$$\text{Scavenging activity (\%)} = \left[ \left( \text{FI}_{\text{control}} - \text{FI}_{\text{sample}} \right) / \text{FI}_{\text{control}} \right] \times 100 \quad (6)$$

in which  $\text{FI}_{\text{control}}$  indicates the fluorescent intensity of the control, while fluorescent intensity of the sample is given by  $\text{FI}_{\text{sample}}$ .

#### 2.12.5. SDS-PAGE

The process of anti-glycation formation applied a method proposed by Zhang et al. [34], who advocated the preparation of 12 % SDS-PAGE under separation on a 30 % polyacrylamide gel which contained 10 % SDS, 1.5 M Tris-HCl buffer pH 8.8, TEMED, 10 % APS, and distilled water. Distilled water was used to dilute the glycated material (5  $\mu\text{L}$ ; 28th day) at 1:30, whereupon bromophenol blue was introduced to the sample in the ratio of 1:5, before denaturing for 5 min at a temperature of 95 °C. The resulting samples (5.5  $\mu\text{g}$  protein) were then separated on SDS-PAGE for a period of 90 min at 120 V. Coomassie blue was used to stain the protein bands, and photographs were taken via ImageQuant LAS 500. Finally, ImageQuant TL v8.1 software was employed to calculate the original-BSA band and glycated-BSA band.

#### 2.13. Statistical analysis

The presentation of all results indicated the mean  $\pm$  standard deviation with data drawn from no fewer than three independent trials, except in specific cases which are clearly stated. One-way analysis of variance (ANOVA) was performed for all data, while Duncan's multiple range test was used to compare differences between samples with the level of  $p < 0.05$  considered significant. All analyses were performed using SPSS 20.0 software (SPSS Inc., Chicago).

### 3. Results and discussion

#### 3.1. Extraction of SGP

##### 3.1.1. Single factor experimentation to optimize SGP extraction

**Fig. 1(A)** presents the outcomes from extractions conducted at different temperatures in the range of 60 °C–100 °C, whereas the other parameters were maintained as an extraction time of 45 min and a water to solid ratio of 25:1 (mL/g). This approach maximized the polysaccharide yield at 5.886 mg/mL when the temperature was 80 °C, confirming the importance of temperature conditions in manipulating the polysaccharide extraction rate. This rate was shown to increase sharply as the temperature rose, but above 90 °C the polysaccharide extraction rate did not change significantly. Temperature changes can alter the water solubility of polysaccharides, while mass transfer is facilitated by extraction time, promoting the release of polysaccharides into the water, and their subsequent diffusion. However, at high temperatures, the polysaccharides tend to be degraded, which has an effect upon the molecular structure [35,36]. Furthermore, higher temperatures represent a waste of energy and resources, and this leads to a lack of economic viability. For the purposes of the response surface analysis, temperatures of 60 °C, 70 °C, 80 °C, and 90 °C were investigated in order to ascertain the optimal value. From **Tables 1** and it can be seen that 80 °C was eventually selected as the central point for further tests.

The study was designed to vary the extraction time to assess the effects upon SGP yields. Durations of 15, 45, 60, and 90 min were used, while the other parameters were maintained as a temperature of 120 °C and water-to-solid ratio of 25 mL/g. **Fig. 1(B)** shows that the SGP extraction yield increased rapidly to a maximum of 6.635 mg/mL at 45 min, whereupon a slow decline in the yield began, clearly revealing the influence of the extraction time upon the extraction yield. If the extraction time is shorter, this may lead to incomplete dissolution of the polysaccharide, whereas a much longer time may result in the degradation of the polysaccharide and accordingly a decline in the product quality. The second stage involved the response surface analysis which used time durations of 35, 40, 45, 50, and 55 min in a narrower range to attempt to establish the ideal extraction time. **Table 1** shows that 45 min was set as the central point for further testing. This was much shorter than the times used in earlier works, which have been in the range of 2–6 h [12, 35,37]. In this study it was believed that a longer duration would not be necessary after the maximum yield had been reached.

The ratio of water to dried sea grape powder has been demonstrated in earlier works to exert a significant influence upon SGP yields. This study therefore investigated different ratios, including 5:1, 10:1, 15:1, 25:1, and 45:1 mL/g of dried algal biomass, and measured the outcomes in terms of polysaccharide yield. The other parameters were fixed at a temperature of 120° and an extraction time of 45 min. **Fig. 1(C)** shows the findings. Interestingly, the SGP yield increased sharply as the ratio of solvent to dried sea grape powder, which began at 1:45, declined to 1:5 mL/g. At 5 mL of water to 1 g of raw dried sea grape powder, the SGP yield was maximized at  $21.704 \pm 0.03$  mg/mL. This can be attributed to the idea that SGP will be diluted when the water volume is higher in proportion to the raw material, and this would reduce the yield [38]. In addition, where a reproduction stage is included in the process of SGP extraction, the extraction time is likely to be extended. When the concentration of SGP molecules rises by placing them in a smaller volume of water, the extraction yield can be increased. In contrast, where the water volume is too small, the SGP become viscous, and the extraction process then becomes much more challenging [21,25]. Accordingly, the selected central point for further experimentation was a water volume of 10 mL.

Earlier studies have sought to find techniques which will increase polysaccharide yields, but these typically require significantly greater energy inputs and expensive equipment, while the extracted materials may suffer degradation during the process, thus altering the bioactive properties and adversely affecting the quality. It is also common for these extraction processes to generate heat to an extent that heat-sensitive compounds will be damaged. One example pertains to a recent study that utilized an RSM-type Box-Behnken design (BBD) to optimize the extraction parameters for polysaccharides obtained polysaccharides from the fruiting body of *Dictyophora*

*indusiata*, a mushroom species. The extraction parameters included a duration of 2.1 h, a temperature of 92 °C, and a solid to liquid ratio of 1:37. The findings of this study provided that the extremely high temperature can degrade the polysaccharide, thus decreasing the yield [39]. However, it was observed that surpassing the temperature threshold sensitive to the extracted polysaccharides could result in their degradation. In contrast, the methodology employed in this study, which relied on water extraction, demonstrated several merits. Firstly, it represented a simplified approach devoid of complexity and the requirement for expensive equipment. Moreover, it could be conducted at lower temperatures and pressures. Furthermore, this approach exhibited swiftness, cost-effectiveness, and reduced energy consumption, thereby enabling a broader range of experimentation [12,40].

### 3.1.2. Predicted model and statistical analysis

Table 2 presents the design and findings for the RSM evaluations which seek to understand the influences exerted by the independent variables in this study. The predicted model was acquired through multiple regression analysis using the data from the experiment, resulting in the second-order polynomial function given as:

$$Y = 1.56 + 0.2469A + 0.0058B - 0.0901 C + 0.0465AB + 0.0232AC + 0.0370BC - 0.1583A^2 - 0.1683 B^2 - 0.2441 C^2 \quad (7)$$

where Y is the predicted value for the percentage yield, and where A = temperature, B = time, and C = water volume.

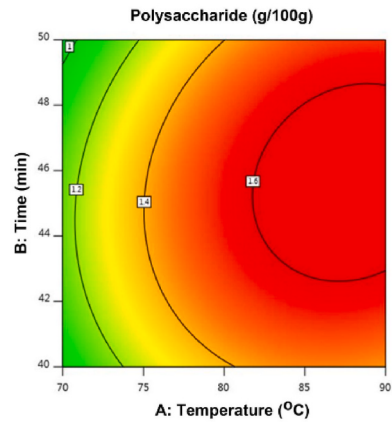
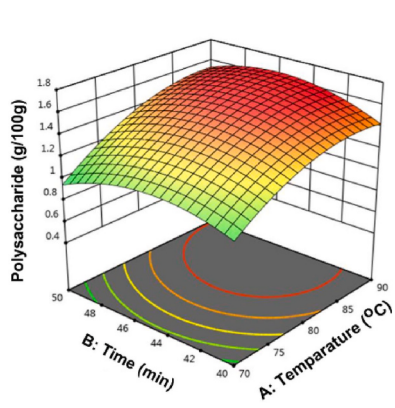
The CCD analysis made use of F-values and P-values as measures of the significance of the various coefficients, whereby a high F-value and small P-value would be indicative of greater significance for the coefficient under investigation. Analysis of variance (ANOVA) was used to evaluate the predictive model and associated variables, while Table 3 shows the results of fitting and the overall statistical analysis. The F-value of the quadratic regression model was high, at 131.27, while the P-value was low ( $P < 0.0001$ ), demonstrating excellent fitness and high significance for the model. For lack of fit, the F-value was 12.30 while the P-value was 0.0769 ( $P > 0.05$ ) which suggested that the lack of fit was not significant. From these findings it can be concluded that the model equation is able to make adequate predictions for the SGP yield under different combinations of values for the input variables. Moreover, the linear coefficients (A and C), interaction coefficient (AB), and quadratic coefficients ( $A^2$ ,  $B^2$ ,  $C^2$ ) were shown to be significant ( $p < 0.05$ ), whereas B, AC, and BC were not significant in terms of their effect upon the yield ( $p > 0.05$ ). The high degree of significance of the model was further confirmed by the values for the determination coefficient ( $R^2 = 0.9941$ ), adjusted determination coefficient ( $R^2_{adj} = 0.9865$ ), predicted determination coefficient ( $R^2_{pred} = 0.9535$ ), and coefficient of variation ( $CV = 4.45\%$ ), which were indicative of suitable accuracy. Were the coefficient of variation to have been higher, this would have suggested greater variation, and thus the response model might be considered unsuitable. When considering the F-values, the effects exerted upon the extraction yield by the various extraction factors can be ordered as  $A > C > B$ , revealing that temperature is more significant than the volume of water, which in turn is more significant than the time. This analysis was further supported by the ANOVA findings, which made use P-values smaller than 0.05 and the regression coefficients which were estimated using the second-order polynomial model designed to explain the SGP yield (Y) which was obtained from Equation (7). The adequate precision ratio for the model, describing the associated error for the predicted response range, was 33.0867, which confirmed the suitability of the model for application in the given design space [41]. The second-order polynomial regression model is shown as Equation (7), and describes the influence of the independent variables upon SGP percentage yield, which served as the response variable. Temperature was shown to have the most significant influence upon the yield, while the maximum yield (1.576 g/100 g) occurred when the temperature was 80 °C, the time was 45 min, and the water volume used was 10 mL/g.

**Table 3**  
ANOVA and estimations of regression coefficients for the yield of polysaccharides using the response surface quadratic model.

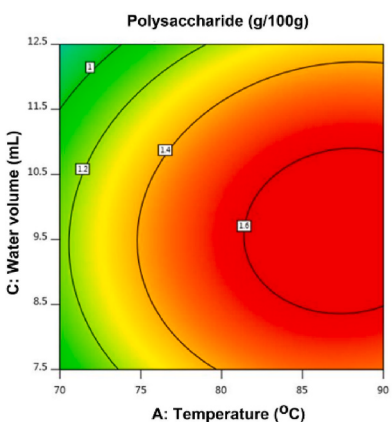
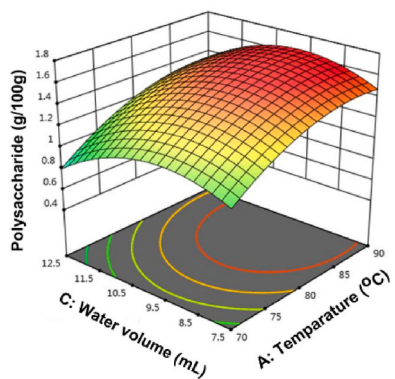
Source	Sum of Squares	df	Mean Square	F-value	P-value	
Model	2.45	9	0.2727	131.27	<0.0001*	significant
A: Temperature	0.9752	1	0.9752	469.46	<0.0001*	
B: Time	0.0005	1	0.0005	0.2547	0.6293	
C: Water volume	0.1300	1	0.1300	62.57	<0.0001*	
AB	0.0173	1	0.0173	8.33	0.0235*	
AC	0.0043	1	0.0043	2.08	0.1923	
BC	0.0110	1	0.0110	5.27	0.0553	
$A^2$	0.4855	1	0.4855	233.74	<0.0001*	
$B^2$	0.5488	1	0.5488	264.19	<0.0001*	
$C^2$	1.15	1	1.15	555.48	<0.0001*	
Residual	0.0145	7	0.0021			
Lack of Fit	0.0141	5	0.0028	12.30	0.0769	not significant
Pure Error	0.0005	2	0.0002			
Cor Total	2.47	16				
Std. Dev.	0.0456					
Mean	1.02					
C.V. %	4.45					
$R^2$	0.9941					
Adjusted $R^2$	0.9865					
Predicted $R^2$	0.9535					
Adeq Precision	33.0867					

\*Variables found to exert a significant effect upon the response ( $p < 0.0001$  or  $p < 0.05$ ).

(A)



(B)



(C)

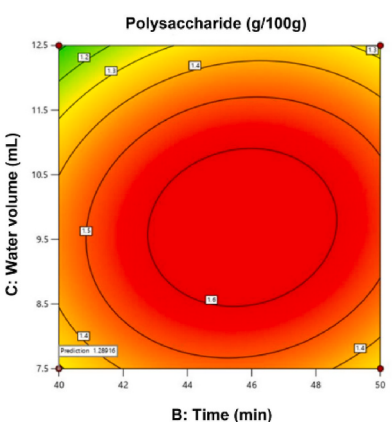
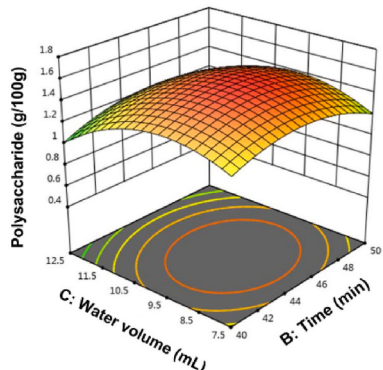


**Fig. 2.** 3D response surfaces and 2D contour plots showing the effects upon SGP yields of independent variable interactions evaluated via the response surface quadratic model measuring the influence of temperature and time (A), the influence of temperature and water volume (B), and the influence of time and water volume (C).

### 3.1.3. Response surface and contour plots

**Fig. 2** presents the 3D response surfaces and 2D contour plots which were employed to illustrate the influence of the different variables which affect the extraction process and polysaccharide yield on the basis of the regression equation. The SGP yield is seen on the z-axis, plotted against two of the independent variables while holding other variables constant at zero. The shape of the contour plot can display the significance of the relationships between interacting variables, whereby a circular plot reveals minimal interaction, and a plot shaped as an ellipse represents important and notable relationships. **Fig. 2(A)** fixes water volume (C) at zero, revealing an increase in SGP yield with rising temperature (A). With an increase in extraction time (B), the initial SGP yield rose sharply, but then began to decline as the variables continued to increase. The resulting contour plot was an ellipse, suggesting that temperature (A) and time (B) had a significant relationship, confirming the data from **Table 2**. When the water volume (C) was held at a low level as shown in **Fig. 2(B)** or at a high level as in **Fig. 2(C)**, there was a decline in the SGP yield. The contour plot was circular, indicating an insignificant interaction between water volume and temperature, and between water volume and extraction time ( $p > 0.05$ ). Design Expert software was then used to establish the optimal conditions for SGP extraction, with the result indicating a temperature of 90 °C, time of 45 min, and water volume of 10 mL. Further experimentation was then carried out to verify the model equation based upon these optimized conditions, resulting in the SGP yield measuring  $1.576 \pm 0.015\%$ . The prediction was a value of 1.655 %, so the experimental result was a close match, presenting a percentage error between the two values of just 4.77 %. This confirms the suitability of the developed regression model to predict SGP extraction yields.

### 3.2. SGP purification

An ion exchange column (DEAE-52 cellulose) was used for the separation of SGP, followed by elution using sodium chloride at differing concentrations in the range of 0.3 M–1.2 M. Fifty fractions of the eluates were gathered, each measuring 10 mL, and three different elution peaks were identified, categorized in **Fig. 3(A)** as SGP<sub>1</sub>, SGP<sub>2</sub>, and SGP<sub>3</sub>. The SGP fractions were separated on the basis of the ionic characteristics they exhibited at differing sodium chloride molarities. These results were different to those achieved for the purification of *C. lentillifera* polysaccharides by Sun et al. [25], since there was a clear affinity for electriferous-polysaccharides displayed by the DEAE-52 cellulose column after the crude polysaccharides entered the column. It was therefore possible to elute the polysaccharides by adjusting the intensity of the sodium chloride to make it stronger, since the ionic force had to be strong enough to elute the fragments. This study revealed the elution of a pair of SGP peaks at 0.3 M and 0.6 M NaCl, whereas the work of Sun et al. [25] produced four peaks at 0.1 M, 0.2 M, 0.8 M, and 1.2 M NaCl. It may be the case that the ionic forces varied in the different salt-soluble components, while differing polar groups may have been present in the chemical structures, accounting for the differences in the findings. Meanwhile, Peng et al. [42] were able to fractionate the aqueous extracts of *Laminaria japonica* with a DEAE-A25

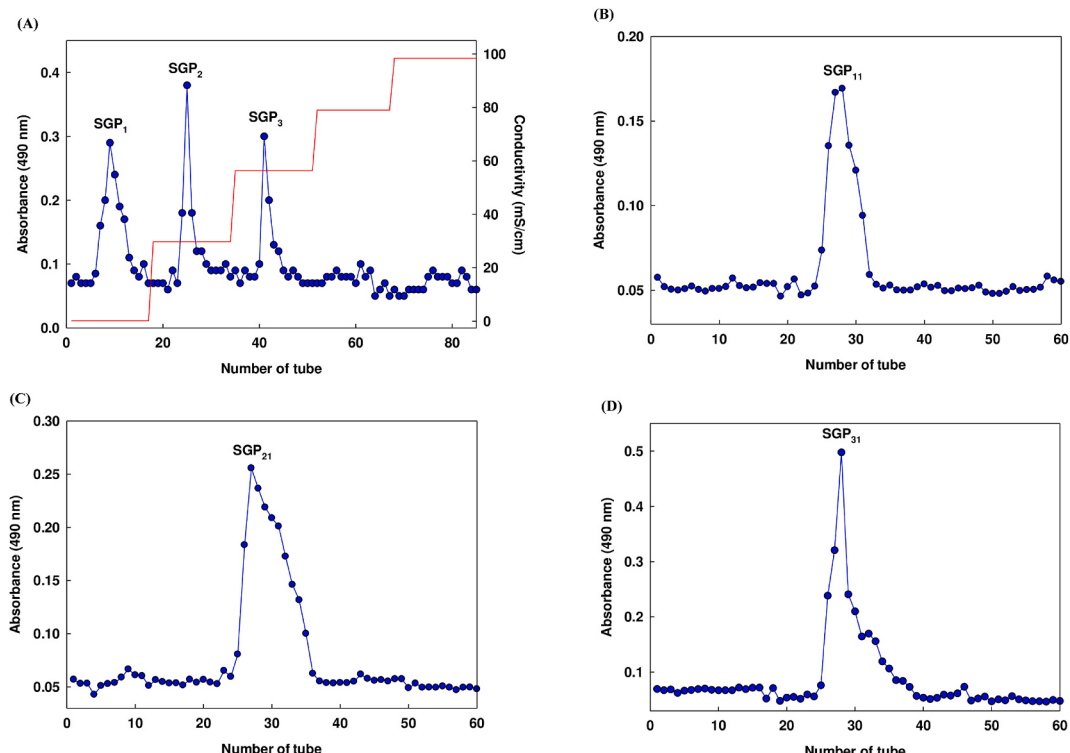


**Fig. 3.** The curve for SGP purification on DEAE-52 cellulose (A), and the elution profile on Sephadryl S-100 column chromatography for SGP<sub>11</sub> (B), SGP<sub>21</sub> (C), and SGP<sub>31</sub> (D).

anion-exchange column to perform gradient elution using 0.7–0.8 mM sodium chloride. The fractions, SGP<sub>1</sub>, SGP<sub>2</sub>, and SGP<sub>3</sub> then underwent purification in a Sephadryl S-100 HR column. The phenol-sulfuric acid method allowed identification of the principal polysaccharide fraction, which was duly collected and labeled as SGP<sub>11</sub>, as shown in Fig. 3(B), while the other fractions were termed SGP<sub>21</sub>, shown in Fig. 3(C), and SGP<sub>31</sub>, shown in Fig. 3(D) with a yield of  $0.37 \pm 0.02\%$ ,  $0.72 \pm 0.01\%$ , and  $0.90 \pm 0.02\%$  from the dried sea grape algae, respectively (Table 4). In order to separate polysaccharides from marine algae, size-exclusion chromatography is a feasible approach since it differentiates by MW [43,44]. In this case, it was possible to purify a sulfated polysaccharide from green algae in a Sephadryl S-300 HR size-exclusion column, before performing enzymatic hydrolysis to produce three fractions which contained oligosaccharides of low MW from a Bio-gel P-4 size-exclusion column [45].

### 3.3. Polysaccharide structure and chemical composition

#### 3.3.1. Chemical compositions and MW

The sulfate content are presented in Table 4 for each of the three fractions, which were also found to comprise 12–22 % sulfate on the basis of the extract weights. These discoveries matched the findings of Sun et al. [22] and Pires et al. [46] whose work examined polysaccharides derived from *Caulerpa*, and their purification. In those works, the polysaccharide fractions were obtained via column chromatography and their sulfate content was in the range of 10–23 %, allowing their categorization as sulfated polysaccharides. HPLC analysis of the sugar content confirmed that there are four neutral sugars which make up the SGPs, as shown in Table 4. The polysaccharides (SGP<sub>11</sub>, SGP<sub>21</sub>, and SGP<sub>31</sub>) were confirmed to be heteropolysaccharides which contained four different monosaccharide types: Glu, Xyl, Man, and GlcA. Although SGP polysaccharides often contain Glu, Man, Xyl, and GlcA, the exact content proportions depend on the conditions under which cultivation took place, with Sun et al. [22] finding *C. lentillifera* polysaccharides comprising 16.8–20.9 % Xyl, 38.7–48.2 % Man, and 33.0–43.2 % galactose (Gal). In contrast, Maeda et al. [24] reported that *C. lentillifera* polysaccharides typically contained Gal (44.2 %) and Xyl (49.3 %), while the quantities of Glu (2.2 %) and uronic acid (4.3 %) were relatively small. Furthermore, Konishi et al. [47] reported a composition ratio for  $\beta$ -1,3 xylan in SGP of Gal:Glc:Xyl:Man as 1.1:4.7:0.3:0.4 (representing 16.9 %, 72.3 %, 4.6 %, and 6.2 % mol, respectively). From the presence of these monosaccharide residues, it can be inferred that SGP<sub>11</sub>, SGP<sub>21</sub>, and SGP<sub>31</sub> are all novel polysaccharides, which are predicted to be glucoxylosemannan and GalA, rather than xylogalactomanans as earlier claimed by Sun et al. [25]. There are compositional differences which might arise as a consequence of the selective separation of the compounds into different salt-soluble components because if the various different polar groups which make up the chemical structure. Differences in the extraction approach and purification techniques might further exacerbate these differences.

After purification via GPC, the MW for each fraction revealed a double peak suggesting a lack of homogeneity among the SGP<sub>11</sub>, SGP<sub>21</sub>, and SGP<sub>31</sub> polysaccharide fractions. Table 4 and Table S1. Figure confirms the mean MWs to be 38.24 kDa, 30.13 kDa, and 30.65 kDa, respectively, in line with the calibration curve of pullulans standards. In this study, the MW was found to be lower than in earlier studies due to the extraction process [48]. In addition to variation stemming from the process of extraction and the different species. The MW of the polysaccharide also affects the antioxidant activity, with low MW polysaccharides (54.7 kDa) derived from green seaweed (*Ulva fasciata*) exhibiting superior antioxidant properties compared to a polysaccharide of greater MW (262.7 kDa) according to Zhong et al. [49]. Confirming this result, Sun et al. [50] examined polysaccharides derived from *L. japonica* and reported that those with a lower MW provided greater antioxidant activity. However, earlier studies have indicated that marine polysaccharides, when possessing specific molecular weights, can exhibit distinct bioactive properties. For instance, research demonstrated that an algal polysaccharide fraction sourced from *Undaria pinnatifida*, having a molecular weight of 130 kDa, significantly enhanced the viability of spleen cells and stimulated the production of IFN- and NO. In contrast, another fraction derived from the same brown seaweed with a molecular weight of 30 kDa displayed reduced activity [51]. Similarly, an algal polysaccharide known as galactofucan from *Saccharina longicurvis*, featuring a molecular weight range of 638–1529 kDa, inhibited the proliferation of fibroblasts. On the other hand, the lower molecular weight fraction (10 kDa) from the same brown seaweed did not affect fibroblast growth or protein secretion [52].

**Table 4**  
Yield, chemical and monosaccharide composition, and molecular weight of purified SGP.

	SGP <sub>11</sub>	SGP <sub>21</sub>	SGP <sub>31</sub>
<b>Yield<sup>a</sup></b>	$0.37 \pm 0.02$	$0.72 \pm 0.01$	$0.90 \pm 0.02$
<b>Chemical characteristics (%)</b>			
Total sugar content	$84.47 \pm 0.07$	$45.86 \pm 0.12$	$77.01 \pm 0.03$
Sulfate content	$12.20 \pm 0.10$	$18.20 \pm 0.21$	$21.80 \pm 0.12$
<b>Monosaccharide composition (%)<sup>b</sup></b>			
Glu	21.98	18.51	20.69
Xyl	17.60	31.73	23.55
Man	18.77	15.89	17.69
GlcA	19.35	16.42	18.25
<b>Average molecular weight (kDa)</b>	38.238	30.133	30.646

<sup>a</sup> Percent weight of the obtained polysaccharide dry weight (% of dry weight).

<sup>b</sup> Percent molar ratio of the sugar residues in the obtained polysaccharide (% of molar ratio). Values are expressed as means  $\pm$  SD ( $n = 3$ ); different.

### 3.3.2. FT-IR analysis

**Fig. 4** and S1 Table present the FT-IR spectra for the purified SGP<sub>11</sub>, SGP<sub>21</sub>, and SGP<sub>31</sub> fractions, revealing the absorption peaks which would normally be seen in polysaccharides throughout the range from 4000 cm<sup>-1</sup> to 515 cm<sup>-1</sup>. In particular, O-H stretching vibration was apparent from the broad and intense peak within the range of 3268.58 cm<sup>-1</sup> to 3355.15 cm<sup>-1</sup>, which was significant since this is a typical absorption feature [53]. C-H stretching vibration was indicated by the absorption recorded at 2932.9–2939.76 cm<sup>-1</sup>, while the stronger absorption peaks measured at 1612.97–1627.76 cm<sup>-1</sup> and 1408.74–1412.02 cm<sup>-1</sup> were caused by the stretching vibration of ionic carboxyl groups (COO<sup>-</sup>), and in particular the symmetrical stretching vibration of C-O and the asymmetrical stretching vibration of C=O in uronic acids [54]. Sulfation groups (SO<sub>3</sub>) were indicated by the absorption peaks at 1225.16–1229.84 cm<sup>-1</sup> and 799.56–817.59 cm<sup>-1</sup> attributed to the symmetrical stretching vibration of C-O-S and the asymmetrical S=O stretching vibration linked to C-O-SO<sub>3</sub>. For all SGP, the FT-IR spectra matched the earlier findings claimed by Sun et al. [25]. Meanwhile, C-S stretching and C=S stretching (sulfides) of sulfates explained the absorption in the range of 577.29–668.73 cm<sup>-1</sup>. The stretching vibration of C-O-C and C-O-H was evidenced by the absorbance observed between 1017.43 cm<sup>-1</sup> and 1020.63 cm<sup>-1</sup>, and provided clear evidence of a pyranose ring. Finally, the absorption at 414–472 cm<sup>-1</sup> was indicative of disulfide S-S stretching. The findings provide affirmation that each of the fractions could be classified clearly as polysaccharides.

### 3.3.3. NMR analysis

In order to obtain important details about the structure of polysaccharides, NMR spectroscopy serves as a convenient and non-destructive method. The NMR data obtained (1D and 2D NMR) can explain the monosaccharide composition and sequences of monosaccharide units, the linkage features, and the presence of  $\alpha$ - or  $\beta$ -type sugars. **Fig. 5(A)** presents the NMR spectra of SGP<sub>11</sub> revealing that  $\alpha$ -glycosidic bonds are prominent in the structure, confirmed by the <sup>1</sup>H signal occurring at 5.25 ppm along with the corresponding <sup>13</sup>C signals observed at 102.35 and 102.47 ppm, which can be seen in the HSQC correlation. In contrast, SGP<sub>21</sub> exhibits notable  $\beta$ -glycosidic bond configurations, made apparent by the <sup>1</sup>H signal at 4.81 ppm along with the <sup>13</sup>C signal at 103.89 ppm observed in the HSQC correlation shown in **Fig. 5(B)**. However, it was difficult to identify the anomeric signals in SGP<sub>31</sub> as a consequence of the signal overlap taking place in the <sup>1</sup>H NMR spectra. Furthermore, a number of the anomeric carbon signals from the <sup>13</sup>C NMR spectra shown in **Fig. 5(C)** could not easily be distinguished from noise. When carefully examined, however, all of the chemical shifts of the C-1 protons were shown not to exceed 5.0 ppm. Anomeric carbons (C-1) accounted for signals observed from 99.17 ppm to 104.24 ppm, while several non-anomeric carbon signals recorded in the range of 60.21 ppm–79.42 ppm matched up to C-2 to C-6 of the sugar residues. These smaller chemical shifts associated with the C-1 protons served to confirm that pyranose rings were present in SGP<sub>31</sub>, connected via  $\beta$ -configuration glycosidic bonds. Earlier work has described variety in polysaccharides derived from

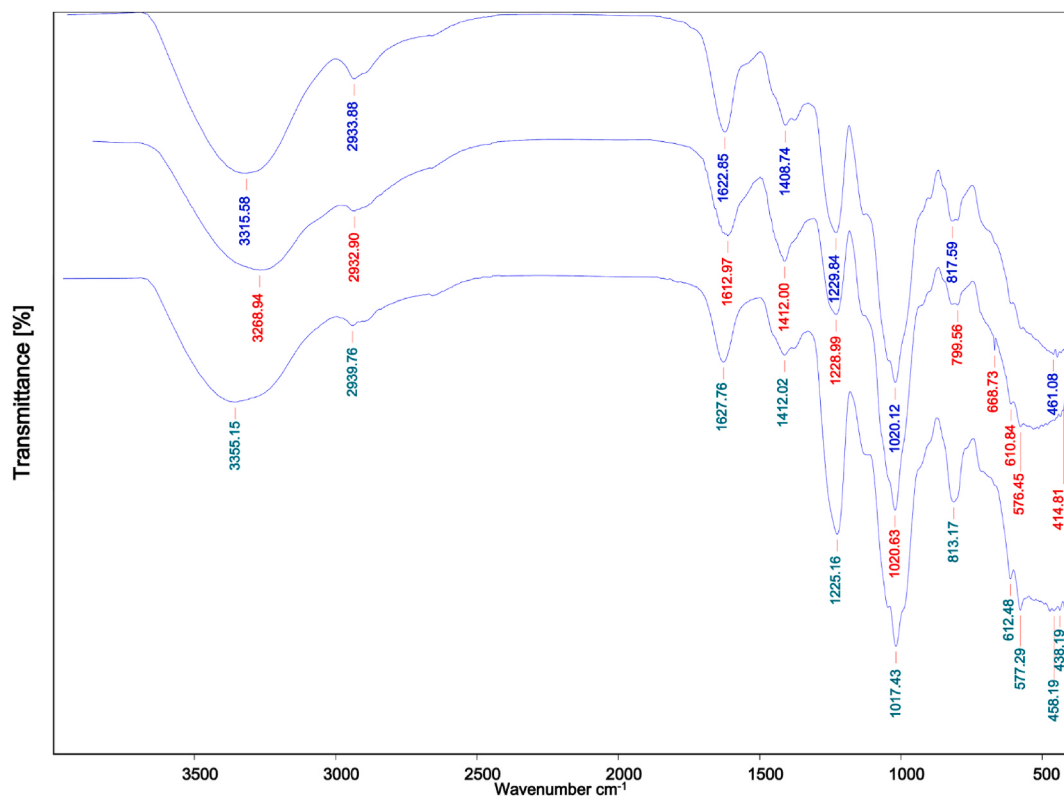


**Fig. 4.** FTIR spectra of SGP<sub>11</sub> (A), SGP<sub>21</sub> (B), and SGP<sub>31</sub> (C).

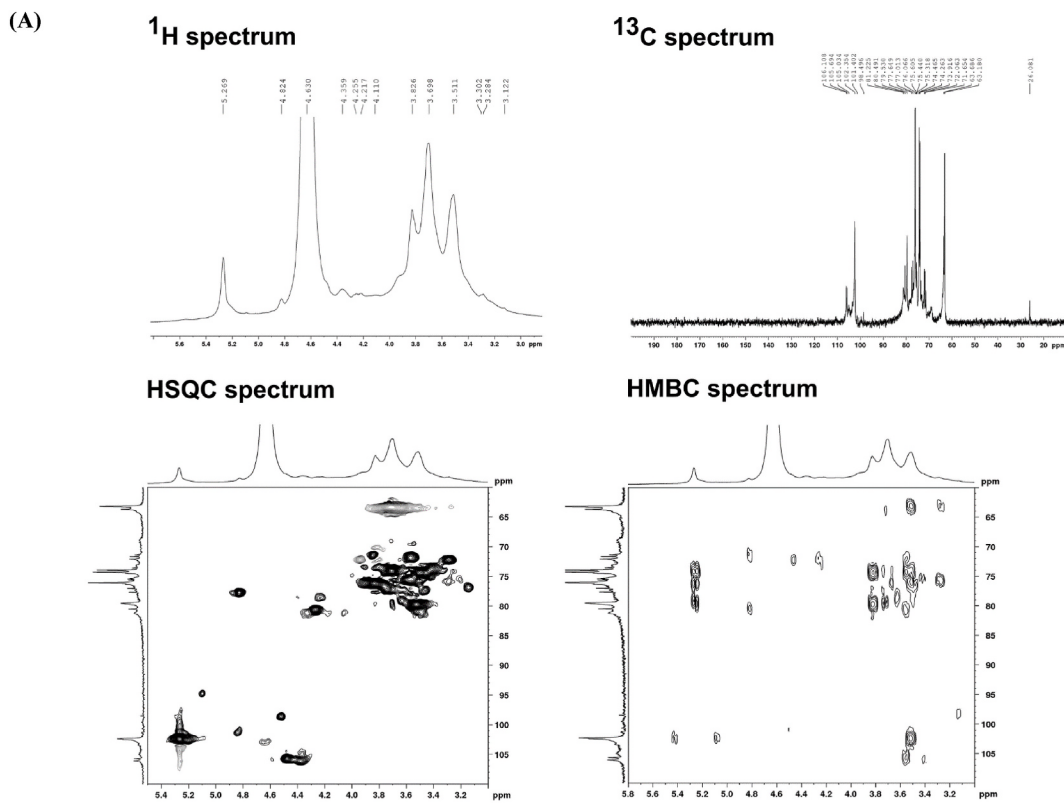


**Fig. 5.**  $^1\text{H}$  NMR spectrum,  $^{13}\text{C}$  NMR, HSQC spectrum, and HMBC spectrum for SGP<sub>11</sub> (A), SGP<sub>21</sub> (B), and SGP<sub>31</sub> (C).

sea grape algae in terms of the chemical composition, with different regions exhibiting different contents, notably involving Xyl, Glu, Gal, and Man [25]. It can thus be argued that the algae habitat affects the chemical composition of the resulting polysaccharides, even from the same species of algae.

### 3.4. Free radical scavenging *in vitro*

When cells are exposed to free radicals, this results in oxidative stress which can damage the cells, causing disease. SGP are of interest in this regard since they offer antioxidant properties and also a high degree of biocompatibility. The DPPH assay offers a means of evaluating the free radical scavenging ability of natural molecules. A methanolic DPPH solution begins as a dark purple color, which clears when antioxidants are introduced, such as aromatic amines, ascorbic acid, tocopherol, or polyhydroxy aromatic compounds. Electron transfer from an antioxidant to ABTS<sup>+</sup> demonstrates the action of ABTS<sup>+</sup> scavenging. Meanwhile, NO will react with oxygen to produce nitrite and proxy nitrite, which are free radicals, leading to inflammation and disease [54,55]. For the SGP<sub>11</sub>, SGP<sub>21</sub>, and SGP<sub>31</sub> fractions, DPPH scavenging activity by  $32.75 \pm 0.05\%$ ,  $22.58 \pm 0.27\%$ , and  $18.41 \pm 0.92\%$  respectively, and ABTS scavenging activity by  $5.39 \pm 0.45\%$ ,  $1.02 \pm 0.02$ , and  $1.28 \pm 0.33\%$  respectively, could only be recorded when the concentration was 31.25 mg/mL, while it was not possible to report IC<sub>50</sub> values for the purified SGP since they lacked the potency to reach the 50 % threshold for scavenging the DPPH, and ABTS<sup>+</sup> radicals. Furthermore, it was found that SGP<sub>11</sub>, SGP<sub>21</sub>, and SGP<sub>31</sub> are able to scavenge NO radicals, depending upon the dose, by  $0.15 \pm 0.04$ ,  $0.34 \pm 0.06$ , and  $0.07 \pm 0.03$  mg/mL respectively. In terms of concentration, the ability of SGP<sub>31</sub> in radical scavenging activity matched that of ascorbic acid, from which it can be inferred that the radical scavenging capabilities of the sulfated polysaccharide were excellent. Carbohydrates display radical scavenging capabilities which might be attributed to the hydrogen supply, since free radicals are able to abstract anomeric hydrogen (1-hydrogen) from carbohydrates, before combining to create neutral molecules [4]. Alkoxyl radicals are able to support the intramolecular hydrogen abstraction reaction which takes place in carbohydrates, leading to a spirocyclization reaction which serves to terminate the radical chain reaction [56]. Strong radical scavenging activity has also been seen in the sulfated polysaccharides obtained from the algae *U. pertusa* [57], *Porphyra haitanensis* [58], and *Laminaria japonica* [59]. In contrast to neutral polysaccharides, sulfated polysaccharides demonstrate much stronger radical scavenging capabilities, despite having a similar structure. This greater scavenging strength might be attributable to the ability of the sulfate group to serve as an electrophile capable of facilitating intramolecular hydrogen abstraction. It was explained by Tsiapali et al. [60] that sulfate groups and phosphate groups, which are both electrophilic substrates, were capable of improving the radical scavenging abilities in carbohydrates. The extent of sulfation and the ability to scavenge free radicals are not directly

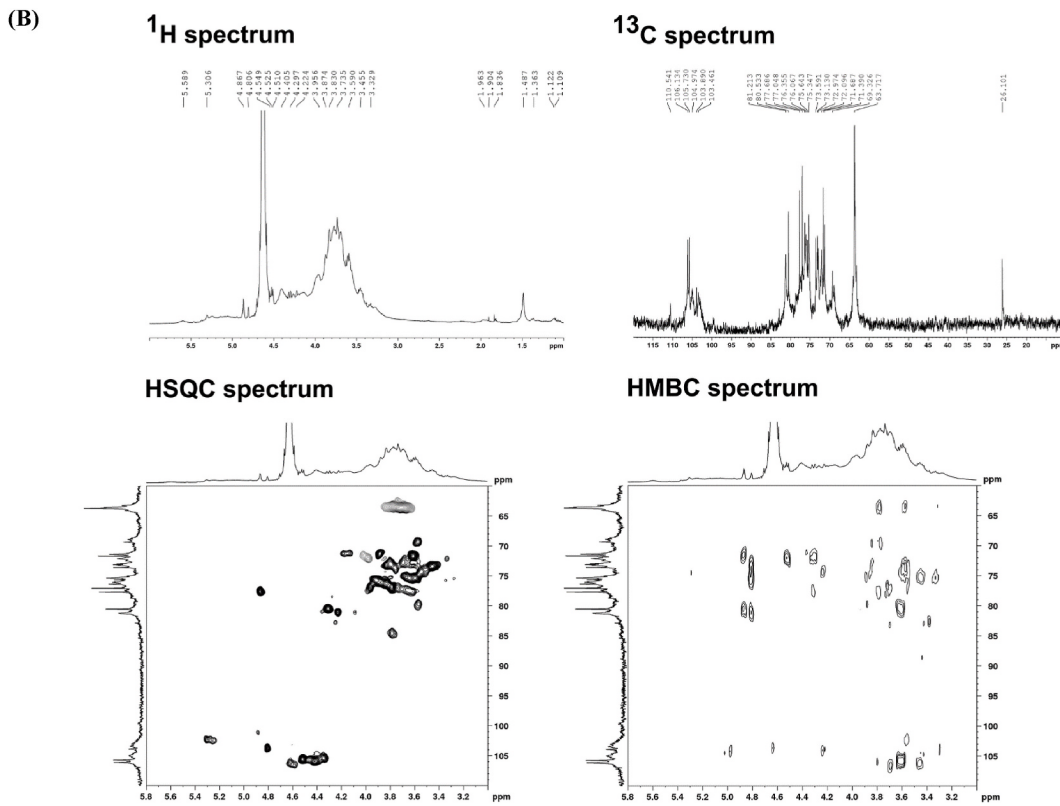
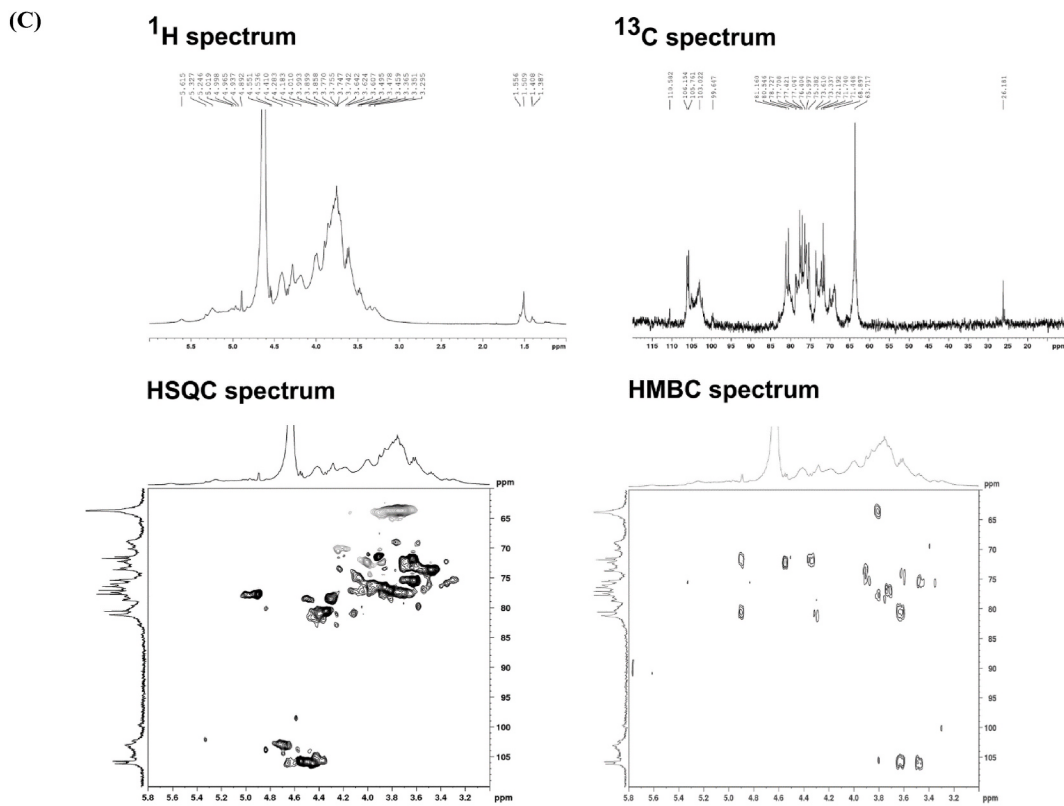


Fig. 5. (continued).

correlated, however, so it would appear that there are other factors which affect the scavenging capabilities of polysaccharides. Earlier research has revealed that the sulfated polysaccharides obtained from algae have both reduction ability and the capacity for DPPH free radical scavenging. For instance, fucoidan F3 derived from *Undaria pinnatifida* has sulfate content of 25.19 % and a MW averaging 27 kDa, yet the DPPH scavenging activity is not especially good, at 68.65 % for 1 mg/mL [61]. In another case, polysaccharides derived from *Sargassum cinereum* offer display high levels of DPPH free radical scavenging ability, with fucoidan isolated from *S. cinereum* achieving a level of 51.99 % for the concentration at 80 µg/mL [62]. Yang et al. [63] experimented to draw comparisons between the sulfated polysaccharide from *Corallina officinalis* and similar de-sulfated polysaccharides in terms of the antioxidant activity, revealing that the sulfated polysaccharides provided superior radical scavenging ability and greater reducing power.

It has recently been shown that polysaccharides of low MW offer more reducing ends capable of reacting with free radical species, and as a consequence their antioxidant activity is found to be greater. In contrast, those polysaccharides which exhibit a lower MW as a consequence of excessive degradation of marine polysaccharides offer reduced antioxidant activity in comparison to the original polysaccharides. Where the MW of a polysaccharide is too low, this may result in an inability to produce an appropriate conformation to ensure that the antioxidant activity is sustained. For example, it has been claimed that a polysaccharide of 9.83 kDa, DHmG-3, which is obtained from the degradation of the 99.7 kDa polysaccharide HmG, has much lower DPPH scavenging activity than the HmG form despite having similar sulfate and sugar content along with the same monosaccharide content [64]. The degradation of fucoidan, with a MW of 38.2 kDa, obtained from *Fucus vesiculosus* produced polysaccharides with MWs of 24 kDa, 15.1 kDa, and 10.3 kDa for differing times. In polysaccharides, as the MW declines, there is a tendency for the DPPH free radical scavenging activity to increase initially, before declining [65]. Zhao et al. [66] found that sulfated polysaccharides with low MW could potentially halt free radical reactions from the beginning, thereby preventing the damage which can be caused by free radicals in excess. The exact nature of the links between the algal polysaccharide structure and the mechanisms of antioxidant activity has yet to be established, however. These results suggest that an appropriate MW can facilitate a polysaccharide to perform better in terms of antioxidant activity, but MW is not consistent across samples, so it would be necessary to investigate single-factor effects in greater details to better understand exactly how MW affects polysaccharides' antioxidant properties.

In the examination of antioxidant activity, one point of interest is that SGP31 demonstrated NO scavenging, in contrast to earlier studies which had placed emphasis primarily upon DPPH and ABTS radicals. As a result, there may be interesting possibilities for SGP<sub>31</sub> in terms of anti-inflammatory activity. NO is a potential mediator of inflammation, which occurs either protectively or detrimentally. The findings in this research concur with those in previous reports which note that sulfated polysaccharides containing fucose (Fuc), Gal, Man, Glu, Xyl, and GalA, display anti-inflammatory properties. Sanjeeva et al. [67], for instance, described the anti-inflammatory capabilities of a sulfated polysaccharide derived from *Sargassum horneri*, comprising Fuc (36.86 %), Gal (30.09 %), Man (11.27 %), and



**Fig. 5.** (continued).

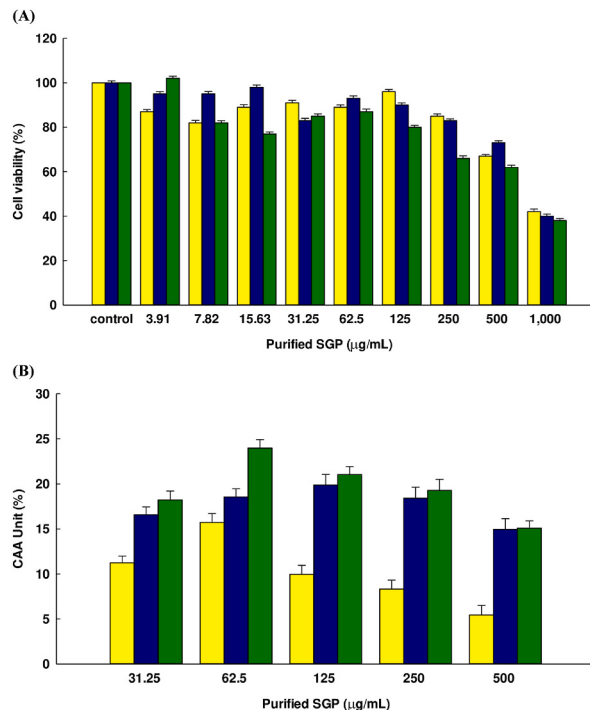


**Fig. 6.** Cell viability of Caco-2 cells after treatment at different concentrations of SGP<sub>11</sub>, SGP<sub>21</sub>, and SGP<sub>31</sub> for 72 h (A), and cellular antioxidant activity of SGP<sub>11</sub>, SGP<sub>21</sub>, and SGP<sub>31</sub> (B). Bars indicate the standard deviation ( $n = 3$ ).

Xyl (7.38 %). Meanwhile, Cui et al. [68] explained that a sulfated polysaccharide derived from *Gelidium pacificum* Okamura also demonstrated anti-inflammatory qualities, and the work of Li et al. [41] presented those anti-inflammatory effects of another sulfated polysaccharide principally comprising Man (30.19 %), Gal (20.10 %), and Glu (18.05 %) [69]. It is thought that anti-inflammatory activity is strongly influenced by the presence of sulfate groups, since similar phenomena have been seen in sulfated polysaccharides including sulfated galactofucan or galactan, and fucoidan, indicating the potential for sulfate groups to serve as polyanions which interact with the positive ions found on cell surfaces as well as modulating intracellular signaling pathways [70].

### 3.5. CAA

Antioxidant properties are typically analyzed via *in vitro* assays, but it is not quite so simple to make accurate predictions of the antioxidant activity within living systems. To address this issue, cell-based assays, such as the CAA assay can be used. Despite the higher cost and lengthier processes, it can sometimes prove beneficial to use human or animal models for evaluation purposes. The CAA assay allows antioxidant capabilities to be evaluated through techniques such as the DCFH method, which is widely used to measure the ability of an antioxidant to protect against DCFH oxidation. In studies of human intestinal absorption and transportation, Caco-2 cells are often used as a model. These human epithelial colorectal adenocarcinoma cells can be investigated as an *in vitro* absorption model, and can also be examined *in vivo* for intestinal absorption. One important area of study has been the intestinal absorption of oral medications, for which the Caco-2 cellular model can make effective *in vitro* predictions. Any antioxidant activity assay making use of Caco-2 cells might therefore provide the advantage of providing insights into the likely intestinal absorption properties of antioxidants. Given that antioxidant ingredients in food products are consumed orally, the intestinal barrier and absorption characteristics become the critical factors affecting functionality. Accordingly, the use of a Caco-2 cellular model might provide improved screening qualities for antioxidant activity in food products and phytochemicals [31,71].

The Caco-2 cell line was used to evaluate the antioxidant activities of the three polysaccharide fractions, SGP<sub>11</sub>, SGP<sub>21</sub>, and SGP<sub>31</sub>. These cells can be used to assess intestinal antioxidant defense, with the results proving comparable to those obtained for *in vitro* models for humans. The MTT assay was used to evaluate the cytotoxic effects of the SGP<sub>11</sub>, SGP<sub>21</sub>, and SGP<sub>31</sub> fractions when varying the concentrations in the range of 3.91 µg/mL to 1000 µg/mL. It was found that the cells were viable in every fraction while the concentration remained below 500 µg/mL, as observed from Fig. 6(A). Accordingly, in the experiments which followed, seaweed extract concentrations above 500 µg/mL were never used. In similar work, Gatea et al. [72] investigated the cytotoxicity of polysaccharide fractions derived from *Phemeranthus confertiflorus* using the Caco-2 cell line, while maintaining concentrations from 3.91 µg/mL to 250 µg/mL, with the results indicating cell viability levels exceeding 80 %. Following incubation for 24 h, the cell viability remained above 80 % throughout the entire range of different concentrations. However, after 72 h, there was notable decrease in viability observed, with the decline directly related to the increasing concentration of the sample. Furthermore, the cytotoxicity levels of the 840.80 µg/mL, 848.21 µg/mL, and 730.03 µg/mL SGP<sub>11</sub>, SGP<sub>21</sub>, and SGP<sub>31</sub> fractions with regard to the Caco-2 cell line were considerably higher when compared to the absence of cytotoxicity observed in the case of normal cells. In the experiment using the polysaccharide from marine microalgae (MMPS), *Synechococcus* sp. VDW, were tested at various concentrations (ranging from 7.81 µg/mL to 1000 µg/mL) and incubated for 72 h. The findings showed that when MMPS concentrations remained below 125 µg/mL, there was no observed cytotoxic effect. However, when concentrations were increased to 250, 500, and 1000 µg/mL, there were corresponding reductions in viable cell numbers by 11 %, 41 %, and 75 %, respectively [28]. Lui et al. [73], it was explained that the concentration of exopolysaccharide (EPS) and sulfated EPS may play a role in governing cell viability and oxidative stress in Caco-2 cells. At higher EPS concentrations, the cell viability declined. There was no significant difference in cell viability ( $p < 0.05$ ) for concentrations ranging from 1 µg/mL to 100 µg/mL in EPS and in sulfated EPS, but differences in viability did become apparent once the concentration for EPS exceeded 200 µg/mL.

The work confirmed that the SGP<sub>11</sub>, SGP<sub>21</sub>, and SGP<sub>31</sub> fractions could play a role in the pre-treatment which served to reduce the DCF fluorescence intensity. Fig. 6(B) presents the findings, indicating similar outcomes for the various concentrations as high as 500 µg/mL for DCF fluorescence intensity ( $p > 0.05$ ) for the SGP<sub>11</sub>, SGP<sub>21</sub>, and SGP<sub>31</sub> fractions. It can therefore be concluded that cellular radical scavenging occurred. These results further demonstrate that all fractions were able to protect the cells from ROS oxidative damage, and therefore these molecules might be suitable candidates for the development of agents capable of preventing ROS formation. This would be potentially advantageous given that ROS production is a cytotoxic process which is associated with various degenerative diseases, and increased ROS concentrations tend to increase the probability of the onset of intestinal pathologies. Accordingly, Caco-2 cells play a useful role as cell culture models when testing transport properties or the bioavailability of drug molecules or nutrients *in vitro*. It is therefore of interest to evaluate the extent to which food antioxidants might serve to protect the intestinal epithelium against damage due to oxidative stress. The *in vitro* approach to research is popular due to its accuracy, affordability, and ability to be repeated or reproduced. Zhang et al. [74], used Caco-2 cells *in vitro* to investigate the transport capabilities of fucoidan sulfate, respectively. The findings revealed differences in transportation within intestinal cells when the structures or physicochemical properties of the polysaccharides differed. The antioxidant effects of SGP are therefore given a scientific basis by the results presented, suggesting that SGP might serve as a natural antioxidant with applications in the treatment of diseases in which oxidative stress is a contributing factor.

### 3.6. Polysaccharide antiglycation

The production of AGEs stems from non-enzymatic reactions which take place when the carbonyl groups in reducing sugars encounter the free amino groups found in proteins. In humans, the non-enzymatic glycation of can lead to arteriosclerosis and diabetic

complications among other chronic conditions [24]. To find potential methods to inhibit glycation, researchers have used the *in vitro* non-enzymatic protein glycation system in attempting to produce biological compounds which offer the required inhibitory properties. This research study, therefore, evaluates the potential for the SGP<sub>11</sub>, SGP<sub>21</sub>, and SGP<sub>31</sub> fractions to inhibit the formation of AGEs in three stages.

### 3.6.1. Influence of purified SGP on NBT reduction

In the early phase of the non-enzymatic glycation process involving proteins, Schiff base and Amadori products are produced. These Amadori products are subsequently able to reduce NBT in alkaline solutions, thereby increasing the yield of the reactant, and achieving the highest level of absorption at 530 nm. Fig. 7(A) presents the glycated-BSA of NBT. In our study, the initial 21-day incubation phase saw a sharp increase in Amadori product content, followed by a more gradual increase before remaining constant as the incubation time increased further. In the initial stages of the glycation reactions, AGEs mediated by free radicals served to convert Amadori products [25], while the NBT reduction due to Amadori products could be inhibited via the incubation of the glucose/BSA system along with the SGP<sub>11</sub>, SGP<sub>21</sub>, and SGP<sub>31</sub> fractions and AG. Each of these fractions demonstrated inhibition, but to a smaller extent than was the case for AG; the following order of effectiveness was recorded for the inhibition of NBT reduction and can be seen in Fig. 8(A): AG > SGP<sub>31</sub> > SGP<sub>21</sub> > SGP<sub>11</sub>. Significant differences among treatments when the concentration was 0.5 mg/mL are also shown in Fig. 7 (A).

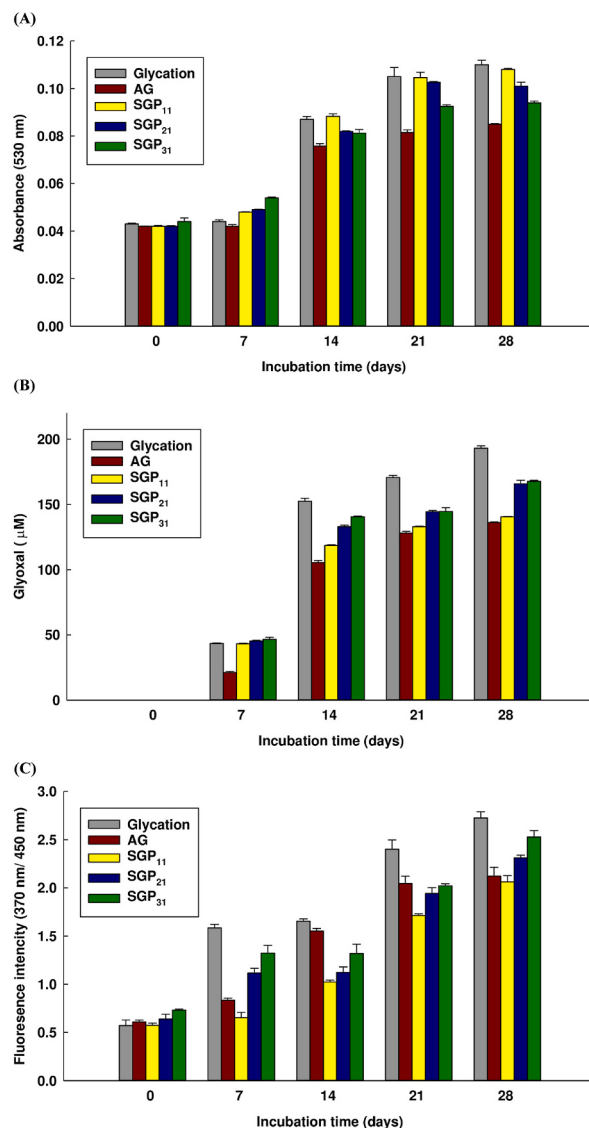


**Fig. 7.** Inhibitive effects of SGP<sub>11</sub>, SGP<sub>21</sub>, and SGP<sub>31</sub> upon AGEs formation (0.5 mg/mL). Inhibition of Amadori product formation (A), inhibition of dicarbonyl compound formation (B), inhibition of AGEs formation (C). Values are shown as mean  $\pm$  SD ( $n = 3$ ).

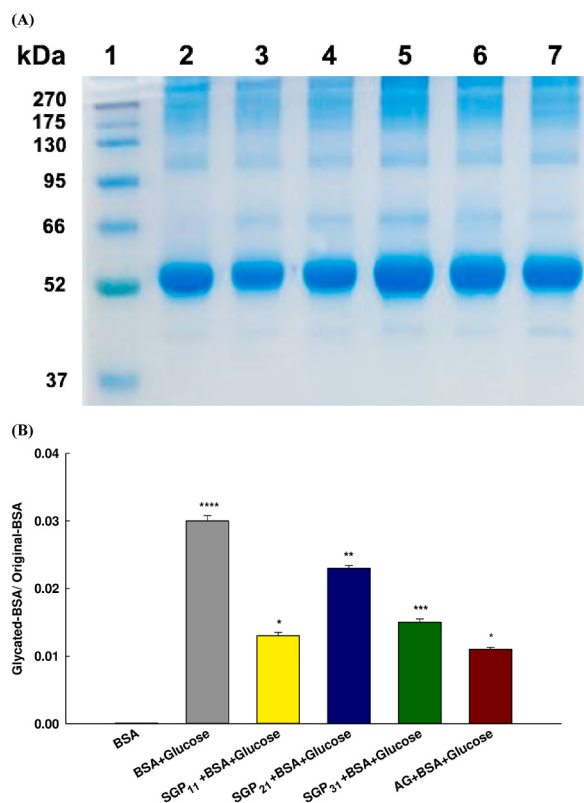


**Fig. 8.** SDS-PAGE profile of glycated protein. (A) Band of SDS-PAGE (1. protein ladder 2. BSA; 3. glycated-BSA; 4. SGP<sub>11</sub>; 5. SGP<sub>21</sub>; 6. SGP<sub>31</sub>; 7. AG (aminoguanidine) (B) analysis of band: glycated-BSA/original-BSA. Bars indicated by different \* represent significant differences in comparison to the negative control (Glycation: BSA + Glucose) and positive control (AG) and at  $P < 0.05$ .

### 3.6.2. Influence of purified SGP on dicarbonyl compounds

A number of previous reports have noted that dicarbonyl compounds are able to promote the rapid cross-linking of proteins and in the intermediate phase will yield stable AGEs. It has been found that almost 50 % of AGEs have their origins in dicarbonyl compounds. In the current study, the initial 21-day period of incubation revealed a sharp rise in dicarbonyl compound content, followed by a more gradual increase, reaching a level which was then maintained steadily. All purified SGP samples along with AG were able to inhibit dicarbonyl compound formation, as shown in Fig. 7(B). The glyoxal content declined with samples showing effectiveness in the following order: AG > SGP<sub>31</sub> > SGP<sub>21</sub> > SGP<sub>11</sub>, so AG delivered the lowest glyoxal content when the concentration was 0.5 mg/mL.

### 3.6.3. Influence of purified SGP on AGE formation

To assess the inhibitory effect upon AGEs formation exerted by the purified SGP, BSA was initially incubated with glucose for 28 days at a temperature of 37 °C, both with and without the purified SGP, while the positive control used was AG. It could be observed from Fig. 7(C) that the fluorescence of the BSA/glucose system increased along with the incubation time, but the fluorescence development of the AGEs was inhibited upon the addition of the purified SGP or AG to the process. In order of inhibitory effectiveness, SGP<sub>11</sub> was stronger than AG, which in turn was stronger than SGP<sub>21</sub>, and SGP<sub>31</sub>, respectively. Notably, the antiglycative activity was a little higher in SGP<sub>11</sub> than in AG. Some studies have argued that the formation of fluorescence is due to oxidation and molecular cross-linking, which typical of AGEs. SGP<sub>11</sub> exhibited the greatest antiglycation activity while significant differences were observed among the different treatments ( $p < 0.05$ ). SGP<sub>31</sub> offered strong antiglycative activity matching that of AG and SGP<sub>21</sub> as a consequence of structural factors, including a lower molecular weight, and also the functional group. Other researchers have noted that polysaccharide antioxidant activity might not be the sole mechanism governing antiglycation, since there was no reported oxidation reaction taking place during the formation of Amadori rearrangement products, while this current study demonstrated that SGP would act upon proteins as an antioxidant and antiglycation agent through all stages. Most notably, SGP<sub>31</sub> presented the greatest antioxidant activity and inhibition of glycation; it has a low MW and high sulfate content, although its performance was lower than that of AG at the start and during the intermediate phase. This matched earlier reports indicating that lower-MW polysaccharides were better able to inhibit free radicals and prevent the formation of AGEs [75,76].

### 3.6.4. SDS-PAGE

The SDS-PAGE profile exhibited one band of glycated-BSA whose MW exceeded the original BSA, as shown in Fig. 8(A). From this it

could be inferred that the period of AGEs formation was associated with cross-linking between proteins and sugars. The quantification of each band was carried out using ImageQuant LAS 500 (GE Healthcare UK Limited, HP7 9NA, UK), while the original-BSA and glycated-BSA bands were determined via ImageQuant TL v8.1 software. Fig. 8(B) shows the intensity ratio for glycated-BSA/original-BSA, while the effectiveness of the samples in inhibiting the formation of AGEs can be ranked to show that SGP<sub>11</sub> and AG were superior to SGP<sub>31</sub>, which was superior to SGP<sub>21</sub> confirming the details of AGEs formation presented in Fig. 7(C). A number of different factors, however, may be responsible for the formation of AGEs, and the production of ROS and free radicals is one important mechanism which can also lead to protein damage in addition to promoting AGEs formation. This research revealed that at concentrations of 0.5 mg/mL, all of the purified SGP can reduce NBT and also exhibit carbonyl formation and offer protection for the thiol groups of protein. This might be attributable to their antioxidant properties and capacity for free radical scavenging and the ability to inhibit the formation of AGEs. While the fraction with the lowest molecular weight, SGP<sub>31</sub>, did not exhibit the greatest ability to prevent the formation of AGEs in the final stage, it was still stronger than SGP<sub>21</sub> and was able to inhibit glycated protein (BSA + glucose). Furthermore, according to Zhu et al. [77], the activity of SGP<sub>31</sub> can be effective during the initial and intermediate stages.

#### 4. Conclusion

In conclusion, this study emphasizes the potential of sea grape algae (*C. lentillifera*) as a rich source of bioactive polysaccharides known as SGP (sea grape polysaccharides). We optimized the extraction process using RSM, resulting in an outstanding yield. Purification yielded three distinct fractions (SGP<sub>11</sub>, SGP<sub>21</sub>, and SGP<sub>31</sub>) with unique characteristics, including molecular weights and glycosidic configurations, containing glucose, galacturonic acid, xylose, mannose, and sulfate groups. From the presence of these monosaccharide residues, it can be inferred that SGP<sub>11</sub>, SGP<sub>21</sub>, and SGP<sub>31</sub> are all novel polysaccharides, which are predicted to be glucoxylomannan and GalA rather than xylogalactomanans. These fractions demonstrated significant antioxidant potential in various *in vitro* assays and cellular antioxidant activity. These findings strongly suggest that SGP<sub>11</sub>, SGP<sub>21</sub>, and notably, SGP<sub>31</sub>, characterized by its low molecular weight and highest sulfate content, exhibit remarkable capabilities in reducing oxidative stress and inhibiting glycation. SGP<sub>31</sub>, in particular, demonstrated the most significant antioxidant activity and glycation inhibition among the fractions, underscoring its potential as a prime candidate for the development of antioxidant-based health products. Nevertheless, it remains essential to conduct *in vivo* studies to thoroughly assess the antioxidant and antglycation activities of SGP<sub>31</sub>.

#### Funding statement

The authors wish to express their sincere gratitude to the Thailand Science Research and Innovation Fund Chulalongkorn University, Thailand (BCG66610030), The 100<sup>th</sup> Anniversary Chulalongkorn University Fund for Doctoral Scholarship (GCUGE11) and The 90<sup>th</sup> Anniversary of Chulalongkorn University Fund (Ratchadaphiseksomphot Endowment Fund (GCUGR1125642019D)). for their financial assistance, without which the completion of this study would not have been feasible.

#### Data availability statement

All data contained within this article.

#### CRediT authorship contribution statement

**Suphaporn Tesvichian:** Writing – review & editing, Writing – original draft, Validation, Methodology, Formal analysis, Data curation. **Papassara Sangtanoo:** Validation, Methodology. **Piroonporn Srimongkol:** Writing – review & editing, Validation, Methodology. **Tanatorn Saisavoey:** Validation, Methodology. **Anumart Buakeaw:** Validation, Methodology. **Songchan Puthong:** Validation, Methodology. **Sitanan Thitiprasert:** Validation, Software, Methodology. **Wanwimon Mekboonsonglarp:** Validation, Software, Methodology. **Jatupol Liangsakul:** Validation, Software, Methodology. **Anek Sopon:** Resources. **Mongkhon Prawatborisut:** Validation, Software, Methodology. **Onrapak Reamtong:** Validation, Software, Methodology. **Aphichart Karnchanatat:** Writing – review & editing, Writing – original draft, Supervision, Project administration, Investigation, Funding acquisition, Formal analysis, Data curation, Conceptualization.

#### Declaration of competing interest

The authors declare that they have no known competing financial interests or personal relationships that could have appeared to influence the work reported in this paper.

#### Acknowledgments

The authors wish to express their gratitude to the Institute of Biotechnology and Genetic Engineering at Chulalongkorn University for the use of the facilities which were necessary in order to complete this research study, and thankful for instrumentation support for 600 MHz Nuclear Magnetic Resonance Spectrometer (NMR) from the Mahidol University-Frontier Research Facility (MU-FRF). In addition, scientists of MU-FRF, Thananya Soonkum, for their kind assistance in instrumental operation and technical supports.

## Appendix A. Supplementary data

Supplementary data to this article can be found online at <https://doi.org/10.1016/j.heliyon.2024.e24444>.

## References

- [1] Y. Yu, M. Shen, Q. Song, J. Xie, Biological activities and pharmaceutical applications of polysaccharide from natural resources: a review, *Carbohydr. Polym.* 183 (2018) 91–101, <https://doi.org/10.1016/j.carbpol.2017.12.009>.
- [2] H. Long, X. Gu, N. Zhou, Z. Zhu, C. Wang, X. Liu, M. Zhao, Physicochemical characterization and bile acid-binding capacity of water-extract polysaccharides fractionated by stepwise ethanol precipitation from *Caulerpa lentillifera*, *Int. J. Biol. Macromol.* 150 (2020) 654–661, <https://doi.org/10.1016/j.ijbiomac.2020.02.121>.
- [3] F. Sultana, M.A. Wahab, M. Nahiduzzaman, M. Mohiuddin, M.Z. Iqbal, A. Shakil, A.A. Mamun, M.S.R. Khan, L. Wong, M. Asaduzzaman, Seaweed farming for food and nutritional security, climate change mitigation and adaptation, and women empowerment: a review, *Aquac. Fish.* 8 (2023) 463–480, <https://doi.org/10.1016/j.aaf.2022.09.001>.
- [4] Y. Fu, H. Jiao, J. Sun, C.O. Okoye, H. Zhang, Y. Li, X. Lu, Q. Wang, J. Liu, Structure-activity relationships of bioactive polysaccharides extracted from macroalgae towards biomedical application: a review, *Carbohydr. Polym.* (2023) 121533, <https://doi.org/10.1016/j.carbpol.2023.121533>, 2023.
- [5] X. Chen, Y. Sun, H. Liu, S. Liu, Y. Qin, P. Li, Advances in cultivation, wastewater treatment application, bioactive components of *Caulerpa lentillifera* and their biotechnological applications, *PeerJ* (2019) e6118, <https://doi.org/10.7717/peerj.6118>.
- [6] L.E. Stuthmann, K. Springer, A. Kunzmann, Cultured and packed sea grapes (*Caulerpa lentillifera*): effect of different irradiances on photosynthesis, *J. Appl. Phycol.* 33 (2021) 1125–1136, <https://doi.org/10.1007/s10811-020-02322-x>.
- [7] J. Sommer, A. Kunzmann, L.E. Stuthmann, K. Springer, The antioxidative potential of sea grapes (*Caulerpa lentillifera*, Chlorophyta) can be triggered by light to reach comparable values of pomegranate and other highly nutritious fruits, *Plant Physiol. Rep.* 27 (2022) 186–191, <https://doi.org/10.1007/s40502-021-00637-6>.
- [8] M. Yangthong, N. Hutadilok-Towatana, W. Phromkunthong, W, Antioxidant activities of four edible seaweeds from the southern coast of Thailand, *Plant Foods Hum. Nutr.* 64 (2009) 218–223, <https://doi.org/10.1007/s11130-009-0127-y>, 2009.
- [9] T. Nagappan, C.S. Vairappan, Nutritional and bioactive properties of three edible species of green algae, genus *Caulerpa* (Caulerpaceae), *J. Appl. Phycol.* 26 (2014) 1019–1027, <https://doi.org/10.1007/s10811-013-0147-8>, 2014.
- [10] N. Syakilla, R. George, F.Y. Chye, W. Pindi, S. Mantihal, N.A. Wahab, F.M. Fadzw, P.H. Gu, P. Matanjun, A review on nutrients, phytochemicals, and health benefits of green seaweed, *Caulerpa lentillifera*, *Foods* 11 (2022) 2832, <https://doi.org/10.3390/foods11182832>.
- [11] S. Fedorov, S. Ermakova, T. Zvyagintseva, V. Stonik, Anticancer and cancer preventive properties of marine polysaccharides: some results and prospects, *Mar. Drugs* 11 (2013) 4876–4901, <https://doi.org/10.3390/foods11182832>.
- [12] J. da Silva Barbosa, L.C.G.F. Palhares, C.H.F. Silva, D.A. Sabry, S.F. Chavante, H.A.O. Rocha, *In vitro* antitumor potential of sulfated polysaccharides from seaweed *Caulerpa cupressoides* var. *flabellata*, *Mar. Biotechnol.* 23 (2021) 77–89, <https://doi.org/10.1007/s10126-020-10004-5>.
- [13] H. Tian, H. Liu, W. Song, L. Zhu, X. Yin, Polysaccharide from *Caulerpa lentillifera*: extraction optimization with response surface methodology, structure and antioxidant activities, *Nat. Prod. Res.* 35 (2021) 3417–3425, <https://doi.org/10.1080/14786419.2019.1700507>.
- [14] A.M. Bayro, J.K. Manluso, R. Alonte, C. Caniel, P. Conde, C. Embralino, Preliminary characterization, antioxidant and antiproliferative properties of polysaccharide from *Caulerpa taxifolia*, *Pharm. Sci. Res.* 8 (2021) 30–36, <https://doi.org/10.7454/psr.v8i1.1102>.
- [15] A.R. Arenajo, A.P. Ybanez, M.M.P. Ababan, C.E. Villajuan, M.R.M. Lasam, C.P. Young, J.L.A. Reyes, The potential anticoagulant property of *Caulerpa lentillifera* crude extract, *Int. J. Health Sci.* 11 (2017) 29–32. PMID: 28936148.
- [16] J.A. Rodrigues, E.S. Vanderlei, L.M. Silva, I.W. Araújo, I.N. Queiroz, G.A. Paula, T.M. Abreu, N.A. Ribeiro, M.M. Bezerra, H.V. Chaves, V. Lima, R.J. Jorge, H. S. Monteiro, E.L. Leite, N.M. Benevides, Antinociceptive and anti-inflammatory activities of a sulfated polysaccharide isolated from the green seaweed *Caulerpa cupressoides*, *Pharmacol. Rep.* 64 (2012) 282–292, [https://doi.org/10.1016/s1734-1140\(12\)07066-1](https://doi.org/10.1016/s1734-1140(12)07066-1).
- [17] Y. Sun, Y. Liu, C. Ai, S. Song, X. Chen, *Caulerpa lentillifera* polysaccharides enhance the immunostimulatory activity in immunosuppressed mice in correlation with modulating gut microbiota, *Food Funct.* 10 (2019) 4315–4329, <https://doi.org/10.1039/C9FO00713J>.
- [18] S. Yoojam, A. Ontawong, N. Lainerd, K. Mengamphan, D. Amornlerdpisorn, The enhancing immune response and anti-inflammatory effects of *Caulerpa lentillifera* extract in RAW 264.7 cells, *Molecules* 26 (2021) 5734, <https://doi.org/10.3390/molecules26195734>.
- [19] H. Ji, H. Shao, C. Zhang, P. Hong, H. Xiong, Separation of the polysaccharides in *Caulerpa racemosa* and their chemical composition and antitumor activity, *J. Appl. Polym. Sci.* 110 (2008) 1435–1440, <https://doi.org/10.1002/app.28676>.
- [20] Y. You, H. Song, L. Wang, H. Peng, Y. Sun, C. Ai, C. Wen, B. Zhu, S. Song, Structural characterization and SARS-CoV-2 inhibitory activity of a sulfated polysaccharide from *Caulerpa lentillifera*, *Carbohydr. Polym.* 280 (2022) 119006, <https://doi.org/10.1016/j.carbpol.2021.119006>.
- [21] N.A. Ribeiro, T.M. Abreu, H.V. Chaves, M.M. Bezerra, H.S. Monteiro, R.J. Jorge, M.M. Benevides, Sulfated polysaccharides isolated from the green seaweed *Caulerpa racemosa* plays antinociceptive and anti-inflammatory activities in a way dependent on HO-1 pathway activation, *Inflamm. Res.* 63 (2014) 569–580, <https://doi.org/10.1007/s00011-014-0728-2>.
- [22] Y. Sun, Z. Liu, S. Song, B. Zhu, L. Zhao, J. Jiang, N. Liu, J. Wang, X. Chen, Anti-inflammatory activity and structural identification of a sulfated polysaccharide CLGP4 from *Caulerpa lentillifera*, *Int. J. Biol. Macromol.* 146 (2020) 931–938, <https://doi.org/10.1016/j.ijbiomac.2019.09.216>.
- [23] K. Khairuddin, S. Sudirman, L. Huang, Z.L. Kong, *Caulerpa lentillifera* polysaccharides-rich extract reduces oxidative stress and proinflammatory cytokines levels associated with male reproductive functions in diabetic mice, *Appl. Sci.* 10 (2020) 8768, <https://doi.org/10.3390/app10248768>.
- [24] R. Maeda, T. Ida, H. Ihara, T. Sakamoto, Immunostimulatory activity of polysaccharides isolated from *Caulerpa lentillifera* on macrophage cells, *Biosci. Biotechnol. Biochem.* 76 (2012) 501–505, <https://doi.org/10.1271/bbb.110813>.
- [25] Y. Sun, G. Gong, Y. Guo, Z. Wang, S. Song, B. Zhu, L. Zhao, J. Jiang, Purification, structural features and immunostimulatory activity of novel polysaccharides from *Caulerpa lentillifera*, *Int. J. Biol. Macromol.* 108 (2018) 314–323, <https://doi.org/10.1016/j.ijbiomac.2017.12.016>.
- [26] M. Dubois, K.A. Gilles, J.K. Hamilton, P.A. Rebers, F. Smith, Colorimetric method for determination of sugars and related substances, *Anal. Chem.* 28 (1956) 350–356, <https://doi.org/10.1021/ac60111a017>.
- [27] A.G. Lloyd, K.S. Dodgson, R.G. Price, F.A. Rose, Infrared studies on sulphate esters. I. Polysaccharide sulphates, *Biochim. Biophys. Acta* 46 (1961) 108–115, [https://doi.org/10.1016/0006-3002\(61\)90652-7](https://doi.org/10.1016/0006-3002(61)90652-7).
- [28] P. Srimongkol, P. Songserm, K. Kuptawach, S. Puthong, P. Sangtanoo, S. Thitiprasert, N. Thongchul, S. Phunpruch, A. Karnchanatat, Sulfated polysaccharides derived from marine microalgae, *Synechococcus* sp. VDW, inhibit the human colon cancer cell line Caco-2 by promoting cell apoptosis via the JNK and p38 MAPK signaling pathway, *Algal Res.* 69 (2023) 102919, <https://doi.org/10.1016/j.algal.2022.102919>.
- [29] T. Saisavoe, P. Sangtanoo, O. Reamtong, A. Karnchanatat, Free radical scavenging and anti-inflammatory potential of a protein hydrolysate derived from salmon bones on RAW 264.7 macrophage cells, *J. Sci. Food Agric.* 99 (2019) 5112–5121, <https://doi.org/10.1002/jsfa.9755>.
- [30] R. Suttisawan, S. Phunpruch, T. Saisavoe, P. Sangtanoo, N. Thongchul, A. Karnchanatat, Isolation and characterization of anti-inflammatory peptides derived from trypsin hydrolysis of microalgae protein (*Synechococcus* sp. VDW), *Food Biotechnol.* 33 (2019) 303–324, <https://doi.org/10.1080/08905436.2019.1673171>.
- [31] K.L. Wolfe, R.H. Liu, Cellular antioxidant activity (CAA) assay for assessing antioxidants, foods, and dietary supplements, *J. Agric. Food Chem.* 55 (2007) 8896–8907, <https://doi.org/10.1021/jf0715166>, 2007.

- [32] X. Wang, L.S. Zhang, L.L. Dong, Inhibitory effect of polysaccharides from pumpkin on advanced glycation end-products formation and aldose reductase activity, *Food Chem.* 130 (2012) 821–825, <https://doi.org/10.1016/j.foodchem.2011.07.064>.
- [33] J.R. Baker, D.V. Zyzak, S.R. Thorpe, J.W. Baynes, Chemistry of the fructosamine assay: D-glucosone is the product of oxidation of Amadori compounds, *Clin. Chem.* 40 (1994) 1950–1955. PMID: 7923778.
- [34] L.S. Zhang, X. Wang, L.L. Dong, Antioxidation and antiglycation of polysaccharides from *Misgurnus anguillicaudatus*, *Food Chem.* 124 (2011) 183–187, <https://doi.org/10.1016/j.foodchem.2010.06.006>.
- [35] M. Zhang, M. Zhao, Y. Qing, Y. Luo, G. Xia, Y. Li, Study on immunostimulatory activity and extraction process optimization of polysaccharides from *Caulerpa lentillifera*, *Int. J. Biol. Macromol.* 143 (2020) 677–684, <https://doi.org/10.1016/j.ijbiomac.2019.10.042>.
- [36] C.P. Passos, A. Rudnitskaya, J.M.M.G.C. Neves, G.R. Lopes, D.V. Evtuguin, M.A. Coimbra, Structural features of spent coffee grounds water-soluble polysaccharides: towards tailor-made microwave assisted extractions, *Carbohydr. Polym.* 214 (2019) 53–61, <https://doi.org/10.1016/j.carbpol.2019.02.094>.
- [37] H. Hao, Y. Han, L. Yang, L. Hu, X. Duan, X. Yang, R. Huang, Structural characterization and immunostimulatory activity of a novel polysaccharide from green alga *Caulerpa racemosa var peltata*, *Int. J. Biol. Macromol.* 134 (2019) 891–900, <https://doi.org/10.1016/j.ijbiomac.2019.05.084>.
- [38] Y. Yuan, Y. Liu, M. Liu, Q. Chen, Y. Jiao, Y. Liu, Z. Meng, Optimization extraction and bioactivities of polysaccharide from wild *Russula griseocarnosa*, *Saudi Pharmaceut.* 25 (2017) 523–530, <https://doi.org/10.1016/j.jsps.2017.04.018>.
- [39] X. Liu, Y. Chen, Y. Wu, X. Wu, Y. Huang, B. Liu, Optimization of polysaccharides extraction from *Dictyophora indusiata* and determination of its antioxidant activity, *Int. J. Biol. Macromol.* 103 (2017) 175–181, <https://doi.org/10.1016/j.ijbiomac.2017.04.125>.
- [40] M.B. Romdhane, A. Haddar, I. Ghazala, K.B. Jeddou, C.B. Helbert, S. Ellouz-Chaabouni, Optimization of polysaccharides extraction from watermelon rinds: structure, functional and biological activities, *Food Chem.* 216 (2017) 355–364, <https://doi.org/10.1016/j.foodchem.2016.08.056>.
- [41] P. Li, L. Zhou, Y. Mou, Z. Mao, Extraction optimization of polysaccharide from *Zanthoxylum bungeanum* using RSM and its antioxidant activity, *Int. J. Biol. Macromol.* 72 (2015) 19–27, <https://doi.org/10.1016/j.ijbiomac.2014.07.057>.
- [42] Z. Peng, M. Liu, Z. Fang, J. Wu, Q. Zhang, Composition and cytotoxicity of a novel polysaccharide from brown alga (*Laminaria japonica*), *Carbohydr. Polym.* 89 (2012) 1022–1026, <https://doi.org/10.1016/j.carbpol.2012.03.043>.
- [43] M. Arman, S.A.U. Qader, Structural analysis of kappa-carrageenan isolated from *Hypnea musciformis* (red algae) and evaluation as an elicitor of plant defense mechanism, *Carbohydr. Polym.* 88 (2012) 1264–1271, <https://doi.org/10.1016/j.carbpol.2012.02.003>.
- [44] G.J. Wu, S.M. Shiu, M.C. Hsieh, G.J. Tsai, Anti-inflammatory activity of a sulfated polysaccharide from the brown alga *Sargassum cristaefolium*, *Food Hydrocolloids* 53 (2016) 16–23, <https://doi.org/10.1016/j.foodhyd.2015.01.019>.
- [45] Y. Yu, Y.P. Li, C.Y. Du, H.J. Mou, P. Wang, Compositional and structural characteristics of sulfated polysaccharide from *Enteromorpha prolifera*, *Carbohydr. Polym.* 165 (2017) 221–228, <https://doi.org/10.1016/j.carbpol.2017.02.011>.
- [46] C.L. Pires, S.D. Rodrigues, D. Bristol, H.H. Gaeta, D.D.O. Toyama, W.R.L. Farias, M.H. Toyama, Sulfated polysaccharide extracted of the green algae *Caulerpa racemosa* increase the enzymatic activity and paw edema induced by sPLA<sub>2</sub> from *Crotalus durissus terrificus* venom, *Rev. Bras. Farm.* 23 (2013) 635–643, <https://doi.org/10.1590/S0102-695X2013005000050>.
- [47] T. Konishi, I. Nakata, Y. Miyagi, M. Tako, Extraction of β-1,3 xylan from green seaweed, *Caulerpa lentillifera*, *J. Appl. Glycosci.* 59 (2012) 161–163, [https://doi.org/10.5458/jag.jag.JAG-2011\\_025](https://doi.org/10.5458/jag.jag.JAG-2011_025).
- [48] S.J. Sun, P. Deng, C.E. Peng, H.Y. Ji, L.F. Mao, L.Z. Peng, Extraction, structure and immunoregulatory activity of low molecular weight polysaccharide from *Dendrobium officinale*, *Polymer* 14 (2022) 2899, <https://doi.org/10.3390/polym14142899>.
- [49] Q.B. Zhong, S. Wei, S. Wang, S. Ke, J. Chen, H. Zhang, H. Wang, The antioxidant activity of polysaccharides derived from marine organisms: an overview, *Mar. Drugs* 17 (2019) 674, <https://doi.org/10.3390/md17120674>, 2019.
- [50] Y. Sun, S. Hou, S. Song, B. Zhang, C. Ai, X. Chen, N. Liu, Impact of acidic, water and alkaline extraction on structural features, antioxidant activities of *Laminaria japonica* polysaccharides, *Int. J. Biol. Macromol.* 112 (2018) 985–995, <https://doi.org/10.1016/j.ijbiomac.2018.02.066>.
- [51] J.Y. Jang, S.Y. Moon, H.G. Joo, Differential effects of fucoidans with low and high molecular weight on the viability and function of spleen cells, *Food Chem. Toxicol.* 68 (2014) 234–238, <https://doi.org/10.1016/j.fct.2014.03.024>.
- [52] L.E. Rioux, V. Moulin, M. Beaulieu, S.L. Turgeon, Human skin fibroblast response is differentially regulated by galactofuran and low molecular weight galactofuran, *Bioact. Carbohydr. Diet.* 1 (2013) 105–110, <https://doi.org/10.1016/j.bcdf.2013.03.004>.
- [53] X. Ji, Y. Cheng, J. Tian, S. Zhang, Y. Jing, M. Shi, Structural characterization of polysaccharide from jujube (*Ziziphus jujuba* Mill.) fruit, *Chem. Biol. Technol. Agric.* 8 (2021) 1–7, <https://doi.org/10.1186/s40538-021-00255-2>.
- [54] V. Lobo, A. Patil, A. Phatak, N. Chandra, Free radicals, antioxidants and functional foods: impact on human health, *Pharm. Rev.* 4 (2010) 118–126, <https://doi.org/10.4103/0973-7847.70902>.
- [55] S. Balyan, R. Mukherjee, A. Priyadarshini, A. Vibhuti, A. Gupta, R.P. Pandey, C.M. Chang, Determination of antioxidants by DPPH radical scavenging activity and quantitative phytochemical analysis of *Ficus religiosa*, *Molecules* 27 (2022) 1326, <https://doi.org/10.3390/molecules27041326>.
- [56] J. Wang, S. Hu, S. Nie, Q. Yu, M. Xie, Reviews on mechanisms of *in vitro* antioxidant activity of polysaccharides, *Oxid. Med. Cell. Longev.* (2016) 5692852, <https://doi.org/10.1155/2016/5692852>, 2016.
- [57] H. Qi, Q. Zhang, T. Zhao, R. Chen, H. Zhang, X. Niu, Z. Li, Antioxidant activity of different sulfate content derivatives of polysaccharide extracted from *Ulva pertusa* (Chlorophyta) *in vitro*, *Int. J. Biol. Macromol.* 37 (2005) 195–199, <https://doi.org/10.1016/j.ijbiomac.2005.10.008>.
- [58] Q. Zhang, N. Li, G. Zhou, X. Lu, Z. Xu, Z. Li, *In vivo* antioxidant activity of polysaccharide fraction from *Porphyra haitanesis* (Rhodophyta) in aging mice, *Pharmacol. Res.* 48 (2003) 151–155, [https://doi.org/10.1016/s1043-6618\(03\)00103-8](https://doi.org/10.1016/s1043-6618(03)00103-8).
- [59] J. Wang, Q. Zhang, Z. Zhang, Z. Li, Antioxidant activity of sulfated polysaccharide fractions extracted from *Laminaria japonica*, *Int. J. Biol. Macromol.* 42 (2008) 127–132, <https://doi.org/10.1016/j.ijbiomac.2007.10.003>.
- [60] E. Tsiapaliki, S. Whaley, J. Kalbfleisch, H.E. Ensley, I.W. Browder, D.L. Williams, Glucans exhibit weak antioxidant activity, but stimulate macrophage free radical activity, *Free Radic. Biol. Med.* 30 (2001) 393–402, [https://doi.org/10.1016/S0891-5849\(00\)00485-8](https://doi.org/10.1016/S0891-5849(00)00485-8).
- [61] W. Mak, N. Hamid, T. Liu, J. Lu, W.L. White, Fucoidan from New Zealand *Undaria pinnatifida*: monthly variations and determination of antioxidant activities, *Carbohydr. Polym.* 95 (2013) 606–614, <https://doi.org/10.1016/j.carbpol.2013.02.047>.
- [62] S.N. Somasundaram, S. Shanmugam, B. Subramanian, R. Jaganathan, Cytotoxic effect of fucoidan extracted from *Sargassum cinereum* on colon cancer cell line HCT-15, *Int. J. Biol. Macromol.* 91 (2016) 1215–1223, <https://doi.org/10.1016/j.ijbiomac.2016.06.084>.
- [63] Y. Yang, D. Liu, J. Wu, Y. Chen, S. Wang, *In vitro* antioxidant activities of sulfated polysaccharide fractions extracted from *Corallina officinalis*, *Int. J. Biol. Macromol.* 49 (2011) 1031–1037, <https://doi.org/10.1016/j.ijbiomac.2011.08.026>.
- [64] J. Mou, C. Wang, Q. Li, X. Qi, J. Yang, Preparation and antioxidant properties of low molecular holothurian glycosaminoglycans by H<sub>2</sub>O<sub>2</sub>/ascorbic acid degradation, *Int. J. Biol. Macromol.* 107 (Pt A) (2018) 1339–1347, <https://doi.org/10.1016/j.ijbiomac.2017.10.161>.
- [65] E. Lahrsen, I. Liewert, S. Alban, Gradual degradation of fucoidan from *Fucus vesiculosus* and its effect on structure, antioxidant and antiproliferative activities, *Carbohydr. Polym.* 192 (2018) 208–216, <https://doi.org/10.1016/j.carbpol.2018.03.056>.
- [66] D. Zhao, J. Xu, X. Xu, Bioactivity of fucoidan extracted from *Laminaria japonica* using a novel procedure with high yield, *Food Chem.* 245 (2018) 911–918, <https://doi.org/10.1016/j.foodchem.2017.11.083>.
- [67] K.K.A. Sanjeeva, I.P.S. Fernando, S.Y. Kim, H.S. Kim, G. Ahn, Y. Jee, Y.J. Jeon, *In vitro* and *in vivo* anti-inflammatory activities of high molecular weight sulfated polysaccharide; containing fucose separated from *Sargassum horneri*: short communication, *Int. J. Biol. Macromol.* 107 (Pt A) (2018) 803–807, <https://doi.org/10.1016/j.ijbiomac.2017.09.050>.
- [68] M. Cui, J. Wu, S. Wang, H. Shu, M. Zhang, K. Liu, K. Liu, Characterization and anti-inflammatory effects of sulfated polysaccharide from the red seaweed *Gelidium pacificum* Okamura, *Int. J. Biol. Macromol.* 129 (2019) 377–385, <https://doi.org/10.1016/j.ijbiomac.2019.02.043>.
- [69] S. Li, N.P. Shah, Characterization, anti-Inflammatory and antiproliferative activities of natural and sulfonated exo-polysaccharides from *Streptococcus thermophilus* ASCC 1275, *J. Food Sci.* 81 (2016) M1167–M1176, <https://doi.org/10.1111/1750-3841.13276>.

- [70] T.U. Jayawardena, K.K.A. Sanjeewa, D.P. Nagahawatta, H.G. Lee, Y.A. Lu, A.P.J.P. Vaas, D.T.U. Abeytunga, C.M. Nanayakkara, D.S. Lee, Y.J. Jeon, Anti-inflammatory effects of sulfated polysaccharide from *Sargassum swartzii* in macrophages via blocking TLR/NF-Kb signal transduction, Mar. Drugs 18 (2020) 601, <https://doi.org/10.3390/nd18120601>.
- [71] M.E. Kellett, P. Greenspan, R.B. Pegg, Modification of the cellular antioxidant activity (CAA) assay to study phenolic antioxidants in a Caco-2 cell line, Food Chem. 244 (2018) 359–363, <https://doi.org/10.1016/j.foodchem.2017.10.035>.
- [72] F. Gatea, E.D. Teodor, A.M. Seciu, Monosaccharides composition and cytostatic activity of polysaccharide fraction of *Phemeranthus confertiflorus* L, FARMACIA 65 (2017) 795–801.
- [73] Z. Liu, L. Dong, K. Jia, H. Zhan, Z. Zhang, N.P. Shah, X. Tao, H. Wei, Sulfonation of *Lactobacillus plantarum* WLPL04 exopolysaccharide amplifies its antioxidant activities *in vitro* and in a Caco-2 cell model, J. Dairy Sci. 102 (2019) 5922–5932, <https://doi.org/10.3168/jds.2018-15831>.
- [74] E. Zhang, E. Chu, L. Xu, H. Liang, S. Song, A. Ji, Use of fluorescein isothiocyanate isomer I to study the mechanism of intestinal absorption of fucoidan sulfate *in vivo* and *in vitro*, Biopharm. Drug Dispos. 39 (2018) 298–307, <https://doi.org/10.1002/bdd.2137>.
- [75] J. Hafsa, K.M. Hamm, M.R.B. Khedher, M.A. Smach, B. Charfeddine, K. Limem, H. Majdoub, Inhibition of protein glycation, antioxidant and antiproliferative activities of *Carpobrotus edulis* extracts, Biomed. Pharmacother. 84 (2016) 1496–1503, <https://doi.org/10.1016/j.biopha.2016.11.046>.
- [76] S. Liping, S. Xuejiao, Z. Yongliang, Preparation, characterization and antiglycation activities of the novel polysaccharides from *Boletus snicus*, Int. J. Biol. Macromol. 92 (2016) 607–614, <https://doi.org/10.1016/j.ijbiomac.2016.07.014>.
- [77] R. Zhu, X. Zhang, Y. Wang, L. Zhang, J. Zhao, G. Chen, J. Fan, Y. Jia, F. Yan, C. Ning, Characterization of polysaccharide fractions from fruit of *Actinidia arguta* and assessment of their antioxidant and antiglycated activities, Carbohydr. Polym. 210 (2019) 73–84, <https://doi.org/10.1016/j.carbpol.2019.01.037>.